Antenna Design and Link Performance Verification of Antennas for 5G mmWave Handheld Devices

NIKHILA CHINNAYANAPALLI RAVI & VINODHINI MYLAI CHANDRASEKARAN
MASTER´S THESIS
DEPARTMENT OF ELECTRICAL AND INFORMATION TECHNOLOGY
FACULTY OF ENGINEERING | LTH | LUND UNIVERSITY

Antenna Design and Link Performance Verification of Antennas for 5G mmWave Handheld Devices

Nikhila Chinnayanapalli Ravi
ni1463ch-s@student.lu.se

Vinodhini Mylai Chandrasekaran
vi5487my-s@student.lu.se

Department of Electrical and Information Technology

Lund University

Supervisor: Anders J Johansson (EIT)

Company supervisor: Bengt Lindoff (BeammWave AB)

Examiner: Michael Lentmaier (EIT)

June 13, 2022

Abstract

The purpose of the thesis is to design a new antenna system and to verify its link performance in 5G FR2 mmWave frequency for handheld devices to enable cellular communication.

The main objective is to design an antenna primarily at 28GHz and 39GHz to enhance spectrum efficiency, along with improved transmission data rates, enabling new cases like Augmented Reality (AR), Virtual Reality (VR) and many more such applications. Here, Ka (27-40GHz) frequency band is used according to IEEE standard.

This objective has been solved by using a rectangular slot to obtain the higher resonant frequency in the patch antenna suitable for use in the real environment. The antenna design modelling and the simulations were done using Altair FEKO Version v2017.20 tool. The required total far field gain is obtained for all the field points specified for the receiving antenna at 28GHz and 39GHz frequency. These results are then fetched in MATLAB based software 'Device antenna radiation visualizer'. The gain and radiation patterns are determined by using the distributed antenna element approach in digital beamforming. The major comparison between the sub-array based analog beamforming and distributed antenna placement in digital beamforming are shown for both 28GHz and 39GHz. Finally, Cumulative Distribution Function (CDF) for Effective Isotropic Radiated Power Transmit power (EIRP) is plotted by assuming random direction of transmission, for each design and for different hand blocking scenarios.

Popular Science Summary

The upcoming 5G-New Radio (NR) Standard will enable cellular communication in the 5G mmWave frequency bands, 24-100GHz. These frequency bands will open for large system bandwidth and tremendously high data rates enabling lots of new use cases, such as smart cities, connected cars, medical applications and much more! Given this cutting-edge technology, exciting challenges arise for today's RF designers that require state-of-the-art solutions.

High isotropic path loss between radio transmitters and radio receivers makes it necessary to rely on antenna arrays with many antenna elements. mMIMO stands for massive Multiple-Input-Multiple-Output. This means using multiple antennas on the same frequency band, with massive indicating a high number of such antennas. Making these antennas directional through mMIMO, the 'beamforming' principle is used to focus the transmission on the direction of the receiving party, may overcome the issues with isotropic path loss.

Traditionally, 5G mmWave has been used more for short-range communication due to its inherent characteristics and propagation loss, but in combination with mMIMO and beamforming it will take the next generations of cellular communication to new levels. Small antennas needed for 5G mmWave open possibilities to integrate the RFIC, front end radio modules, filters, and antenna element in a single RF chip. This fact, in combination with 5G-NR is standardized for communication also over 5G mmWave radio frequencies which enables mmWave communication in smartphone and IoT devices, will drastically change the way beamforming will be implemented in mobile devices in the future[1],[2],[3].

In our Master Thesis, we propose a dual band single polarized patch antenna design for the 5G mmWave frequencies and obtain gain and radiation patterns for the required frequencies at 28GHz and 39GHz that are further simulated in a MATLAB link level simulator to analyze the performance of 5G mmWave handheld devices in a non- stationary radio environment to obtain an omnidirectional coverage in desired directions.

Acknowledgement

Table of Contents

List of Figures

x

List of Tables

List of Abbreviations

2D	2 dimensional
3D	3 dimensional
3GPP	3rd Generation Partnership Project
5G	5th Generation Cellular Network Technology
ADC	Analog-to-Digital Converter
AR	Augmented Reality
BF	Beamforming
CAD	Computer Aided Design
CEM	Computational ElectroMagnetics
CDF	Cumulative Distribution Function
DAC	Digital-to-Analog Converter
dB	decibel
dBi	decibel isotropic
dBm	decibel milliwatts
E-Field	Electric Field
EIRP TX	Effective Isotropic Radiated Power Transmit power
EM	ElectroMagnetics
EMC	ElectroMagnetic Compatibility
FR2	Frequency Range 2
FR4	Flame Retardant
GHz	Giga Hertz
H-Field	Magnetic Field
IoT	Internet of Things
mMIMO	Massive Multiple Input Multiple Output
mmWave	Millimeter Wave
MoM	Method of Moments
NR	New Radio
PA	Power Amplifier
PCB	Printed Circuit Board
RF IC	Radio Frequency Integrated Chip
SNR	Signal to Noise Ratio
UE	User Equipment
UL	Uplink
VR	Virtual Reality

Introduction

_____

In the evolving world of communication system technologies, the recent 5G-NR standard advancements in the 5G mmWave frequency bands, primarily at 24-30 GHz and 37-43 GHz, sound promising in providing features like enhanced spectrum efficiency along with improved transmission data rates, enabling new cases like VR, AR and many such applications. The requirement to rely upon the antenna arrays consisting of many antenna elements therefore becomes vital, due to the existence of a high isotropic path loss between the radio transmitter and the radio receiver. With the aid of antenna arrays, a high directional gain can be obtained through beamforming techniques, thereby overcoming the path loss. In this way, the transmitter- receiver pair makes use of the antennas to obtain a good amount of energy in a specific direction. These antenna arrays overcome the path loss by high directional gain through beamforming.

The principles behind 5G mmWave beamforming applied to a 5G-NR can be explained as follows. A base station – mobile device communicates via directing the radio signal towards each other using many antenna elements at both transceiver sides. A typical number of antenna elements for 5G mmWave communication in 5G could be 64-256 antenna elements in a radio base station and 4-16 antenna elements in a mobile device. For smartphones and IoT devices targeting the mass market, the radio architecture needs to be optimized from cost and size perspective. An illustration of the principle is shown in Figure 1.1.

The start-up company BeammWave is developing digital beamforming architecture, by integrating the RF IC, front end Radio modules, filters, and antenna elements in a single RF chip that will drastically change the way beamforming will be implemented in mobile devices in the future, which will be based on digital beamforming [1],[2],[3].
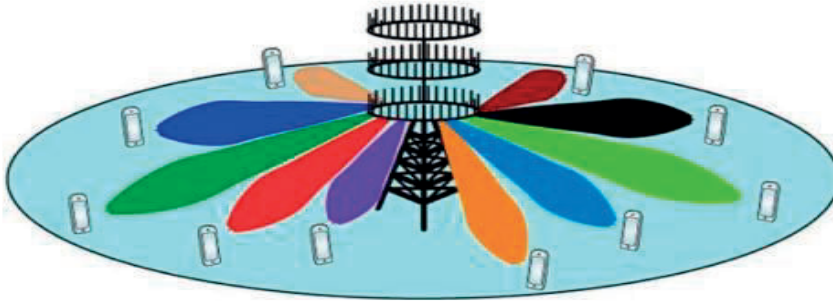
Figure 1.1: Illustration of Beamforming between radio station and mobile devices. **Source:** [1]

Figure 1.2 below represents the existing analog beamforming solution used by Qualcomm (on the left) and BeammWave's proposed digital beamforming architecture (on the right) [5]. The analog beamforming architecture is embedded with 8, 4x2 antenna panels of size 25x18 mm² and the digital beamforming architecture consists of front-end modules, filters, RF IC and antenna element that are integrated in a single RF chip of size 3x3 mm². With respect to size, the total footprint (PCB) for analog and digital beamforming architectures are 3600 mm² and 144 mm² respectively.
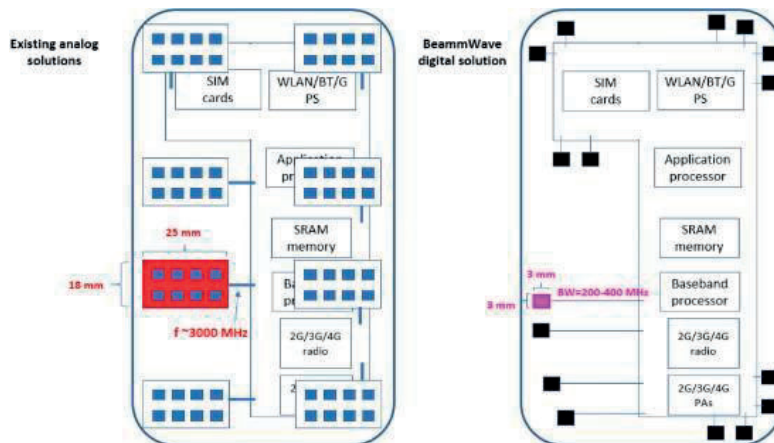
Figure 1.2: Beamforming in mobile devices. **Source:** [3]

1.1 Goal of project

The aim with this Master thesis is entailed as follows.

a. A pre-study and a thorough background study of 5G mmWave radio technology, antenna design, analog and digital beamforming architectures and beam management control principles.

b. Design of the 5G mmWave antenna that supports NR FR2 ranges (28 GHz and 39 GHz) using Altair FEKO version v2017.20 antenna design tool, thereby ensuring and aiming to develop an antenna design that suits the digital beamforming architecture.

c. The designed 5G mmWave antenna will be later used in a MATLAB link level simulator, that helps simulate the 5G mmWave handheld device performance in a non-stationary radio environment. This is performed to verify how well the designed antenna performs on a link level simulator.

d. Finally, the thesis is finalized with a report describing the antenna design principles, radiation patterns, accompanied by the analysis and findings from simulations.

Background & Motivation

_____

The thesis is started with the key motivation of modifying the way of implementing beamforming in mobile devices in the near future, that could be digital based. As we may know, the first generation 5G mmWave smartphones use sub-array based analog beamforming architecture as explained in Figure 1.2.

The proposed distributed antenna placement in a digital beamforming architecture is relatively less bulkier when compared to the current sub-array based analog beamforming solution, with the former having the footprint of 144 mm^2 and the latter being 3600 mm^2. The distributed antenna element in digital beamforming solution for 5G mmWave will open up for antenna placement flexibility by combining the antenna elements from different directions. Simulation tools are needed to control, to analyze the antenna diagram and the resulting beamforming. These will be performed with 5G mmWave RF chip placement on the footprint mentioned.

To incorporate this distributed antenna element in digital beamforming method, the key step is to design an antenna that supports 5G mmWave frequency band. The main advantage of using 5G mmWave frequencies is that it will offer large blocks of continuous radio spectrum and therefore helps overcome the bandwidth congestion problem at sub 6GHz frequency bands. Furthermore, the small wavelength for 5G mmWave acts as an advantage in making small and compact radio transceiver antennas for mobile phones [1],[2],[3].

With the prime intention to understand the requirements and challenges in designing a 5G mmWave frequency band antenna, an extensive study has been done to formulate design calculations and parameters, to obtain a feasible yet compact patch antenna design with an acceptable gain and radiation patterns.

Definitions & Parameters

According to IEEE, the antenna is defined as '**That part of a transmitting or receiving system that is designed to radiate or to receive EM waves**'.

Antenna characteristics:
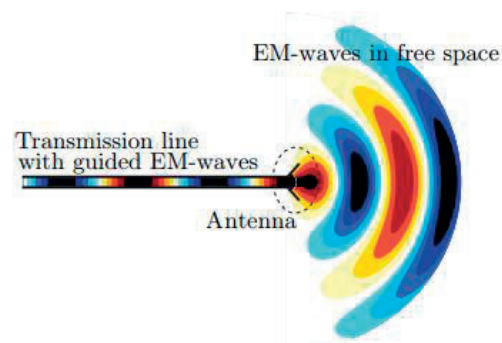
Figure 3.1: Antenna characteristics. **Source:** [6]

The signal carried by the transmission line should be accepted by the antenna element and should not reflect back. The accepted signal should be transformed to EM waves. Finally, the radiated EM wave should propagate in the direction of the receiver [6].

In order to begin with the design of any form of an antenna, it is significant to define the fundamental parameters. With reference to [7], the design values for the patch antenna proposed are evaluated using the definitions and parameters explained throughout this chapter.

3.1 Antenna input impedance

Input impedance is defined as the ratio of voltage and current at the pair of input and output antenna terminals [7]

$$Z = \frac{V}{I},$$

$$(3.1)$$

where,
V = voltage at the antenna terminal
I = current at the antenna terminal

3.2 Relative permittivity

This parameter can be defined as the ratio of absolute permittivity of a medium to the absolute permittivity of vacuum, that can be expressed as in [7], shown below

$$\varepsilon_r = \frac{\varepsilon}{\varepsilon_0},$$

$$(3.2)$$

where,
ε_0 = permittivity of vacuum (8.854×10^{-12}[F/m])

3.3 Reflection coefficient

The EM wave (signal) on the transmission line to be accepted by the antenna. This requires that the reflection coefficient $|\Gamma|$, is small as in [7], shown below

$$\Gamma = \frac{(Z_{in} - Z_0)}{(Z_{in} + Z_0)},$$

$$(3.3)$$

where,
Γ = voltage reflection coefficient at the input terminal of the antenna
Z_{in} = antenna input impedance
Z_0 = characteristic impedance of the transmission line

3.4 Antenna Efficiency

The efficiency of an antenna can be defined as the ratio of radiated power to the input power. This infers that, for an antenna to be highly efficient, an enormous amount of the input power must be radiated. On the contrary, the antenna efficiency is considered low, if most of its input power is stored back in the form of losses or reflected (probably due to impedance mismatch) [7].

Typically, the theoretical efficiency ranges from 0 to 1. Therefore, the total antenna efficiency e_0 can be calculated as

$$e_0 = e_r \times e_c \times e_d \, , \tag{3.4}$$

where,
e_r = reflection efficiency
e_0 = total efficiency
e_c = conduction efficiency
e_d = dielectric efficiency

3.5 Far Field Region

In this region, the EM fields are dominating by the radiating field. The E and H fields are orthogonal to each other and to the direction of propagation as with plane waves. The below equation is used for far-field region

$$\text{Far Field region} > \frac{2D^2}{\lambda} \, , \tag{3.5}$$

where,
D = Maximum linear dimension of the antenna
λ = Wavelength of the EM waves

Antennas are used to transfer signals at large distances in the far field region. Usually, the measurements in the far field region taken when the distance from the antenna is much greater than the size of the antenna and the wavelength [7].

3.6 Radiation Pattern

The radiation pattern can be defined as the variation of the power radiated by an antenna as a function of the direction away from the antenna. This power variation as a function of the arrival angle is observed in the antenna's far field [7].

3.7 Antenna Gain

The parameter 'gain' for an antenna can be defined by measuring the amount of power that is transmitted in the peak radiation's direction relative to that of an isotropic antenna source [7]. In other words, the gain of an antenna can be defined as 4π times the ratio of the maximum radiation intensity in each direction to the total input power accepted by the antenna [8]

$$\text{Gain}\,(\theta, \phi) = 4\pi \left[\frac{Radiation\ Intensity}{Total\ input\ power} \right] = 4\pi \left[\frac{U(\theta,\phi)}{P_{in}} \right] \, , \tag{3.6}$$

3.8 Antenna Directivity

The directivity of the antenna is defined as the ratio of maximum power density to its average value over a sphere as observed in the far field of an antenna.

In other words, an antenna has different radiation or reception patterns in various directions, antenna directivity is the parameter describing how much the radiation pattern of the antenna is directional [7].

$$\mathrm{D}(\theta, \phi) = \frac{U(\theta, \phi)}{P_{ave}},$$ (3.7)

where, the radiation intensity normalized by the isotropic (average) intensity

$$P_{ave} = \frac{P_{rad}}{4\pi}.$$

Patch Antenna Design Calculations

_____

In the previous chapter, the definitions and the parameters required for antenna designing were elaborated. This chapter explains how the designing of patch antenna was formulated.

Patch antenna, also known as Microstrip antenna is exceedingly useful in cellular phones as it is cost-effective, easy to fabricate that can be printed onto the board [8]. The patch antennas are widely used for many applications, where the size, weight and cost are the major constraints. The rectangular patch (radiating element) is primarily a metallic patch that is etched on top of the dielectric substrate chosen. The chosen dielectric substrate is sandwiched between the radiating patch and the ground plane. This is explained in the Figure 4.1 below [9].
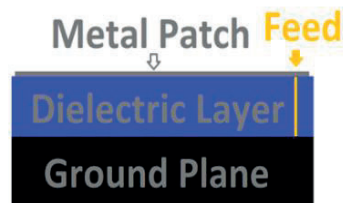
Figure 4.1: Structure of the patch antenna

To start with the design, one would primarily require the frequency(s), dielectric constant and substrate material with its thickness. Therefore, the design requirements are stated as follows.

- Resonant frequencies = 28GHz and 39GHz
- Bandwidth Requirement = 24.5GHz to 29GHz and 37.5GHz to 43GHz
- Dielectric constant ranging from 3 – 5
- Tangent loss ranging from 0.001 – 0.004 approx. (1% to 20% loss)
- Substrate thickness to be less than 1mm
- Maximum size of the antenna = 4 x 4 mm
- Acceptable return loss = 6dB

From the above mentioned requirements, one of the options to start the antenna designing would be that this is a dual band antenna that needs to have its resonances in Ka bands n260, n261 with the bandwidth ranges 37GHz-40GHz and 27.50GHz-28.35GHz respectively [10]. With the help of the above mentioned parameters, the antenna design calculations are explained ahead.

4.1 Selection of dielectric constant

With respect to dielectric constant of the substrate, in general, the substrate can be chosen that has a dielectric constant ranging between $2.2 \leq \varepsilon_r \leq 12$ [9]. As per the design requirements mentioned above, we chose FR-4 substrate with dielectric constant of 4.67, and substrate thickness of 0.8 mm, as referred from [11].

4.2 Design calculations

In this section, the antenna design calculations are presented. To begin with, the shape of the patch antenna chosen is rectangular, as it is a widely used shape for design of wideband antennas operating in 5G mmWave bands or microwave bands [11]. The rectangular patch antenna length and width is represented by L and W. The input reactance of the patch is zero, because the antenna resonates exactly when the length is used as half a wavelength. In the designing process the L and W are finite and will change based on the fringing effect. There will always be a fringing effect on the edges of the patch antenna, which makes the effective length more than the physical length calculated. This fringing effect depends on the length, width of the patch antenna and on the thickness/height of the substrate.

To illustrate the design methodology in an easier approach along with accurate results, we may consider starting with the transmission-line model [9].

Starting with the design calculations, the width of the patch W_p evaluates as

$$W_p = \frac{c}{2fo\sqrt{\frac{\varepsilon_r+1}{2}}} \quad , \qquad\qquad (4.1)$$

where ε_r = 4.67 chosen, which is the relative permittivity of the dielectric substrate, f_0 is the resonant frequency (28GHz) and **c** is the speed of light in vacuum.

The length of the patch L_p is obtained by,

$$L_p = L_{eff} - 2\Delta L \,, \tag{4.2}$$

where,

$$L_{eff} = \frac{c}{2fo\sqrt{\frac{\varepsilon_r+1}{2}}} \,, \tag{4.3}$$

where f_0 is the resonant frequency (39 GHz) and ΔL in Eq [4.2] can be defined as,

$$\Delta L = 0.412h\,\frac{(\varepsilon_{eff}+0.3)(\frac{Wp}{h}+0.264)}{(\varepsilon_{eff}-0.258)(\frac{Wp}{h}+0.8)} \,, \tag{4.4}$$

In Figure 4.2 below, ΔL is called the fringing length, meaning that the dimensions of the patch along its length are extended on each end by a distance ΔL [9]. The fringing length is also the function of the width to height ratio and the effective dielectric constant.
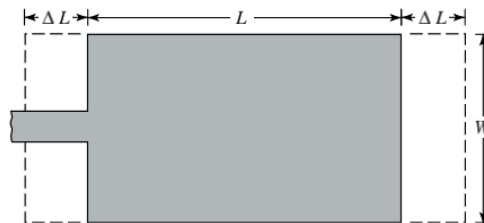
Figure 4.2: Rectangular patch antenna. **Source**: [9]

Here **h** is the thickness of the substrate (=0.8 mm), ε_{eff} is the effective relative constant and can be obtained as follows. Most of the electric field lines travel on the substrate but some also travel via air. The effective dielectric constant is constant for lower frequencies and with intermediate frequencies, its values start to monotonically increase and ultimately reaches the actual values of dielectric constant of the substrate [9], this means that the electric field lines now travel in the substrate. The starting values mentioned for lower frequencies can be referred to as the static values of the effective dielectric constant that is given by,

$$W/h > 1,$$

$$\varepsilon_{eff} = \frac{\varepsilon_r + 1}{2} + \frac{\varepsilon_r - 1}{2} \left[\frac{1}{\sqrt{1 + \frac{12h}{Wp}}} \right], \qquad (4.5)$$

Finally, the length and width of the ground plane are calculated as shown below

$$Lg = 6h + Lp \qquad\qquad (4.6)$$

$$Wg = 6h + Lp, \qquad\qquad (4.7)$$

In our design, we considered the length 'Ls ' and width 'Ws' of the substrate to be as equal as the ground plane dimensions, stated in Eq [4.6] & [4.7]. Therefore, Ls = Lg and Ws = Wg [11].

All the calculated values from the above equations have been implemented in the Altair FEKO antenna design tool, which is explained ahead in Section 4.3 of this chapter.

4.3 Feeding techniques

The patch antenna needs to be fed with an input power using feeding techniques. There are 4 types of feeding techniques to feed a microstrip patch, which are coaxial feed/probe feed, inset feed (edge or line feed), proximity-coupled feed and aperture-coupled feed.

In this project, the requirement was to feed the input power from the bottom of the patch antenna and therefore the options were coaxial feed and aperture-coupled feed. Inset feed involves the usage of a conducting microstrip line directly attached to the patch antenna. Proximity feed requires two substrates generally and this was easily ruled out for our design. Since the coaxial feed is preferably easy to start with, this method was first chosen, where the inner conductor of the coaxial cable is connected to the patch antenna and outer conductor of the coaxial cable to the ground plane. This is explained in the Figure below [12].
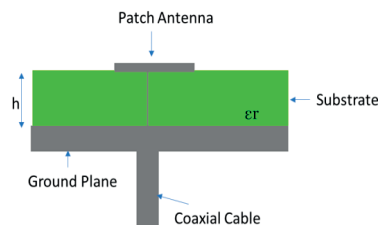
Figure 4.3: Patch antenna with coaxial feeding technique

Position of the coaxial feed on the patch mainly determines the input impedance. The diameter of the probe feed is also considered to have some effects on matching; however, it is usually considered to be thin enough to travel the current along its length. The feeding position where the impedance matches 50 Ω is given by moving the coaxial feed on the patch [12].

Antenna Designing Tool

5.1 Introduction to Altair FEKO

From previous discussions so far, the patch antenna is modelled using the software called FEKO which is made by the company Altair. Altair FEKO is leading antenna simulation tool, which is used for high frequency EM simulations. FEKO is a method of moments (MoM) tool that is used to calculate radiation pattern, gain, impedance, mutual coupling between the antennas and the electric current that flows on an antenna.

The basic flow of Altair FEKO analysis starts with building a wire to represent a geometry of an antenna. Secondly, the geometry support structure should be constructed, which in turn affects the antenna performance. Then, the created antenna and its surrounding geometries have to be meshed. Second last, the requested solution types and setting solution parameters should be chosen in CADFEKO or EDITFEKO. Finally, the FEKO solver is executed, and results are viewed in POSTFEKO [9].

5.2 Antenna in product development

First the antenna should be designed for the given requirement, in this project we used the patch antenna with finite ground plane. The antenna is designed using Computational ElectroMagnetics (CEM) tool and radiation pattern is computed. Then the designed antenna is placed on the mobile phone and the radiation pattern is computed together with the mobile phone. Finally, in the results obtained (discussed in Chapter 9) it is evident that the maximum, minimum radiation pattern differs due to the internal interaction on the mobile phone. As the last step, virtual mobile test is conducted by placing the antenna on the mobile phone in a distributed way.

5.3 Introduction to MoM

The MoM is classified as full wave solutions with source method, where the full wave solutions solve Maxwell Equations accurately without making any assumptions regarding the nature of electromagnetic problems and provide reliable results with good Computer Aided Design (CAD) model as well as the mesh. The mesh is available for the designed CAD model, which is used to capture the geometry and suitable for frequency of operations. In the source method, will solve for integral form of Maxwell's Equations. The source method is used to solve the electric and magnetic currents, in terms of discretization (mesh) it is done for surfaces with segments and triangles and finally, the radiation boundary problems are also taken care in this source method by using free space Green's Function.

_____Chapter **6**

Designing the Microstrip Patch

6.1. Initial design models: Dual band patch antenna

6.1.1 Patch antenna with single feed pin

With the help of all the definitions stated, the patch antenna was designed in the CADFEKO antenna design software tool, which is intended for the analysis of a wide range of electromagnetic problems like EMC analysis, antenna design, dielectric media, cable modelling and many more [9].

As a first thought to design the patch antenna in CADFEKO, we incorporated all the theoretical values found from Section 4.1 and designed a patch antenna that looked as follows.
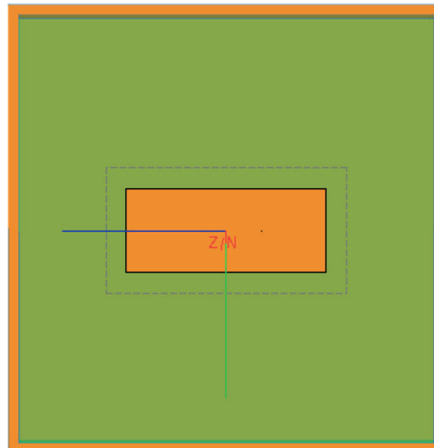
Figure 6.1: Initial dual band patch antenna design with 1 feed pin on X axis

The variables used for designing the above patch are as follows:
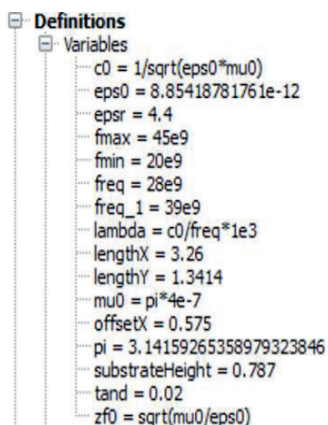
Figure 6.2: Design variables for the initial dual band patch antenna

From Figure 6.2, **fmax** and **fmin** are the start and end frequencies (defined in Hz) that help obtain the simulated results for the entire continuous (interpolated) range defined. **freq** and **freq_1** are the resonant frequencies desired. The variables **lengthX** and **lengthY** are the width and the length of the patch antenna respectively. **OffsetX** and **OffsetX_1** are the coaxial feed pins. tanδ is the dielectric loss tangent [9].

The geometry for the rectangular patch antenna modelled in the tool can be expressed as shown in Figure 6.3 below.
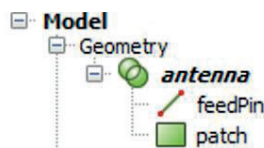
Figure 6.3: Geometry of the antenna model

The geometry for the feedpin along with the start and end point, as well as the geometry for the patch along with base centre, width, depth are shown in Figure below.

Figure 6.4: Geometry of feed pin and patch antenna

With this design, we obtained resonances at 21.18 GHz and 40.79 GHz, which is far away from the required resonant frequencies.
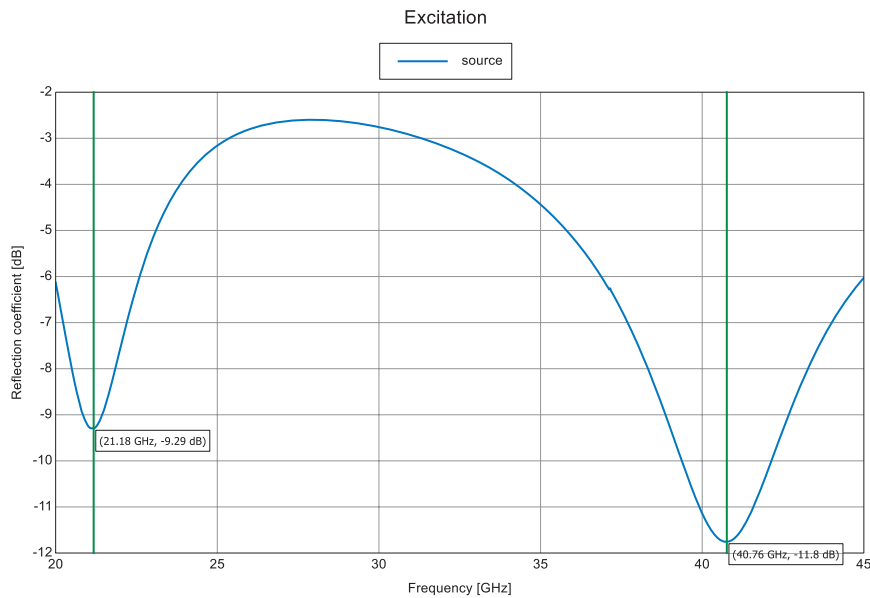
Figure 6.5: Resonances at undesired frequencies

The patch parameters are changed based on resonant frequency, return loss and bandwidth. Those patch parameters are lengthX and lengthY.

Therefore, extensive research was made to design an antenna that resonates at the desired 28 GHz and 39 GHz. Hence, with reference to the paper [11], an inverted-L slot was designed, which is discussed in the next sub-section.

6.1.2 Patch antenna with an Inverted-L slot

The design with an inverted-L slot was constructed and the model looked as shown in Figure 6.6. Two feed pins were introduced on the X and Y axis (90 degrees to each other) with an intention to excite the current surface paths and thereby, resonate at the desired frequencies. The slot introduced vertically (with reference to X-axis) helps in altering/tweaking the resonant frequencies, whereas the slot that sits horizontally (with reference to Y-axis) caters to some amount of bandwidth enhancement.
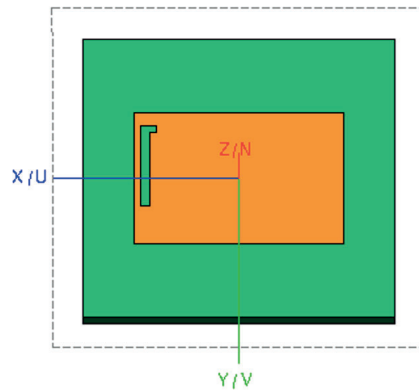
Figure 6.6: Inverted-L slot for dual band patch antenna design with 2 feed pins

The variables used for designing the Inverted-L slot patch are as follows:

Figure 6.7: Design variables for the inverted L-slot dual band patch antenna

The geometry for the Inverted-L slot patch antenna modelled in the tool is shown in Figure 6.8 below.

Figure 6.8: Geometry of the antenna model

The geometry for the feedpins along with the start and end point, as well as the geometry for the vertical and horizontal L slot along with basecorner, width, depth are shown in Figure 6.9 below.
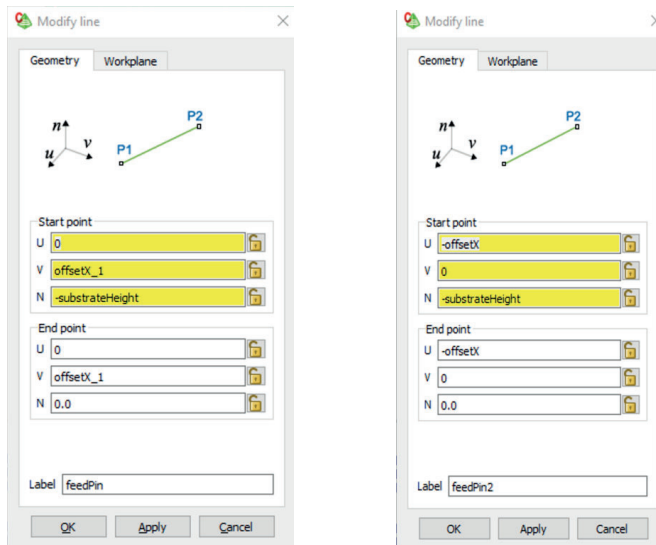
Figure 6.9: Geometry of feed pin and patch antenna

Figure 6.10: Geometry of Horizontal and Vertical slots

This antenna model helped us obtain the desired resonant frequencies and the simulation results shown below in Figure 6.11 proves the same.
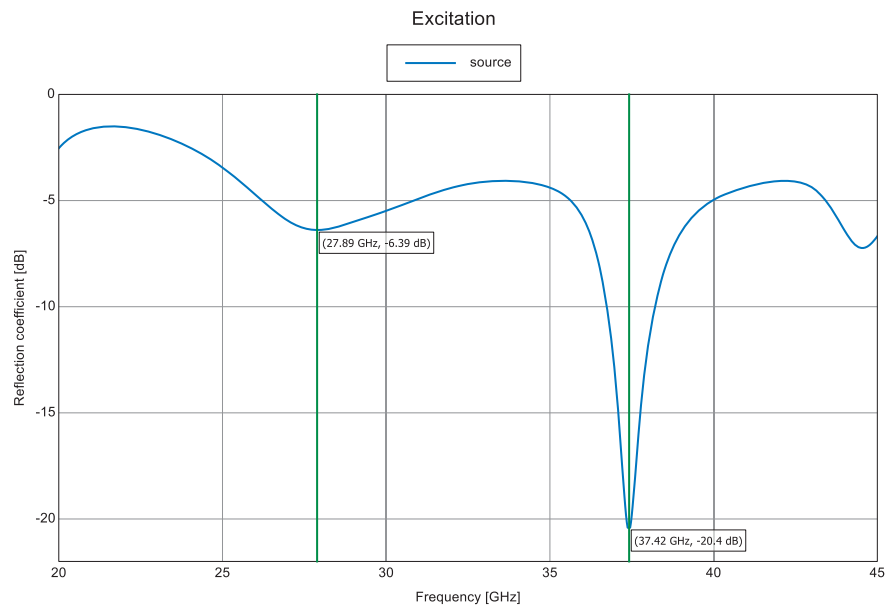
Figure 6.11: Resonances obtained close to the desired frequencies with 2 feed pins

Now, it was clear to us that the inverted-L slot suits our design requirements. Once the resonant frequencies were obtained, our next task was to verify for a good impedance matching and finally the antenna gain. With this design, the initial impedance was not well-matched, where we obtained at 65 Ω & 68 Ω for 28 GHz and 39 GHz respectively. Therefore, efforts were made to bring down the values closer to the input port impedance 50 Ω by moving the 2 feed pins closer to the center of the patch.

As a design engineer, it is always advantageous to think about the ease of the fabrication process ahead. Employing fabrication methods like Fabric-based embroidered antennas (they affect efficiency and shifts the resonant frequency) or Polymer Embedded antennas (they affect efficiency due to the loss of tangents of the polymers) impose difficulties in the antenna performances, as long as "Inkjet Printing, Screening and Photolithography" method is enforced, which is a fast antenna prototyping technique with ease of producing complex antenna models [13].

Since we have an inverted L-slot, it could be slightly complex to perform precision cutting of the patch antenna unless the photolithographic fabrication method is incorporated. Therefore, we experimented with just one vertical slot (with reference

to X-axis) and omitted the horizontal slot and yet, we obtained acceptable and good results. Further details on this design are explained in the next section.

6.2. Proposed and final model: Dual band patch antenna

With the previous learnings and experiments, the proposed antenna design model for this thesis is elaborated in this section.

The final design model of dual band patch antenna with one vertical slot and 2 feed pins is depicted in Figure 6.12 below.
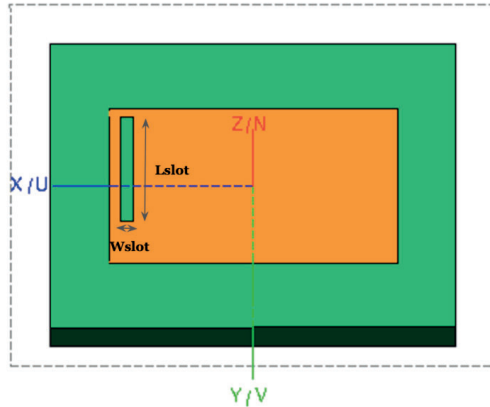
Figure 6.12: Dual band patch antenna with one vertical slot and 2 feed pins.

The length (Lslot) and width (Wslot) of the slot is calculated as 0.7Lp and 0.046Wp respectively. Figure 6.12 illustrates the unmeshed CADFEKO model along with the calculation requests [9]. The variables used for designing the rectangular slot patch are shown in Figure 6.13 below.
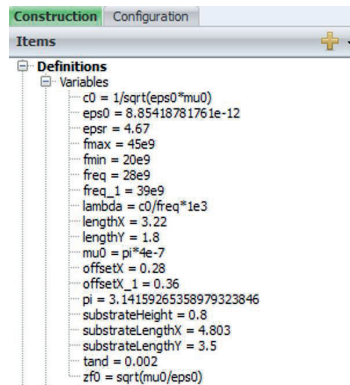
Figure 6.13: Design variables for the proposed dual band patch antenna

The geometry for the rectangular slot patch antenna modelled in the tool is shown in Figure 6.14 below.
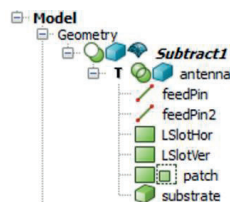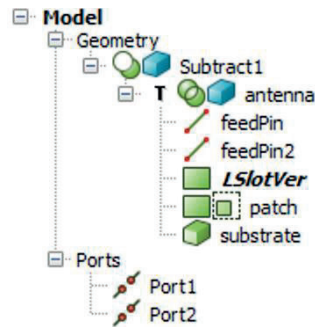

Figure 6.14: Design model parameters with wire ports

The geometry for the feed pins along with the start and end point, as well as the geometry for the vertical slot along with base centre, width, depth are shown in Figure 6.15 and Figure 6.16 below.
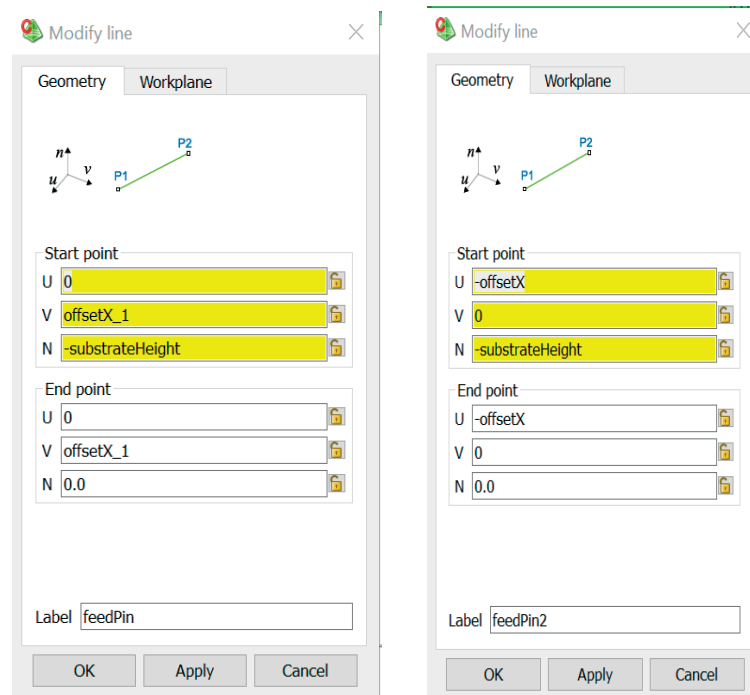
Figure 6.15: Geometry of the 2 feed pins
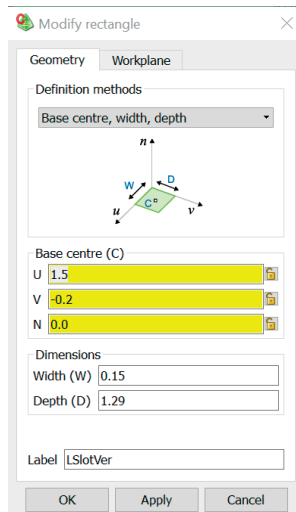
Figure 6.16: Geometry of the vertical slot

6.3 Meshing Information

Meshing is performed as a step after the design modelling is completed. The need to 'mesh' the design model/geometry in order to obtain a discretized representation, which is used by the FEKO solver to obtain the requested calculations. The MoM technique is used to reduce the Maxwell equation to an integral equation, then approximating the integral via discrete chunks over the space. Finally, a mesh grid up the design i.e., create triangles so that the solver uses them to obtain the required solutions [9]. Below Figure 6.17 represents how meshing is performed.
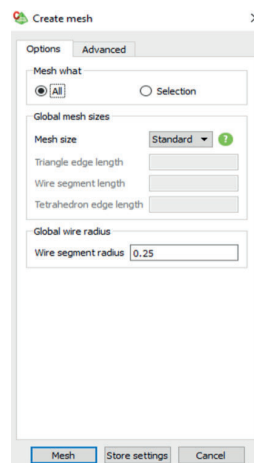
Figure 6.17: Mesh properties

Here, the standard auto-mesh settings are used with the **wire segment radius** equal to 0.25 [9]. Since the design model contains wire ports, defining the radius for the same is a mandate. Post meshing, the whole design model is divided into triangles as shown in Figure 6.18 below.
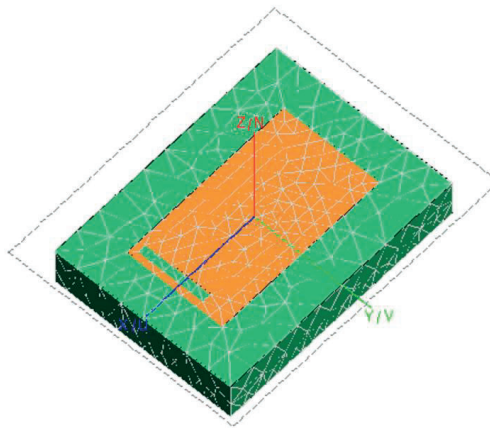
Figure 6.18: Meshed antenna model

6.4 FEKO Solver

With the meshed model in hand, the next step is to run and validate the model. As a thoughtful step before running, it is always advisable to check the **Symmetry** settings as shown in Figure 6.19 below.
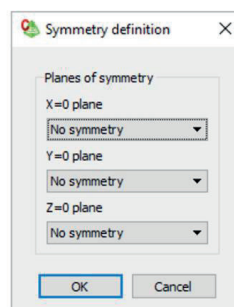
Figure 6.19: Symmetry definition

Since the model is not symmetric on X axis & Y axis due to the presence of slot, it is important to choose 'No symmetry' option, failing to do the same would result in simulation warnings throughout, as shown in Figure 6.20 below.

Warning 16224: Mesh model is not symmetric for the following reasons:
    Errors in symmetry around the X=0 plane:
        Subtract1.Face92 breaks the symmetry definition. Either it does not have a symmetrical counterpart, or it is not symmetrical around the plane.
        Subtract1.Face8 breaks the symmetry definition. Either it does not have a symmetrical counterpart, or it is not symmetrical around the plane.
        Subtract1.Wire147 breaks the symmetry definition. Either it does not have a symmetrical counterpart, or it is not symmetrical around the plane.
        Subtract1.Face4 and Subtract1.Face7 have a different number of mesh elements.
    Errors in symmetry around the Y=0 plane:
        Subtract1.Face92 breaks the symmetry definition. Either it does not have a symmetrical counterpart, or it is not symmetrical around the plane.
        Subtract1.Face8 breaks the symmetry definition. Either it does not have a symmetrical counterpart, or it is not symmetrical around the plane.
        Subtract1.Wire17 breaks the symmetry definition. Either it does not have a symmetrical counterpart, or it is not symmetrical around the plane.

Figure 6.20: Warning message due to Symmetry definitions

The results are to be obtained by adding an impedance load to port 2, terminated with 50 Ω of load as shown in Figure 6.21 below.
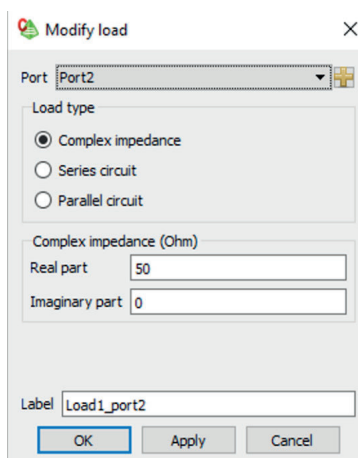
Figure 6.21: 50 Ω load added to port 2

Here, the **complex impedance** load type is chosen, which is a frequency independent load that consists of constant real and imaginary parts. This load type can be applied to wire, edge or transmission line ports [9]. Furthermore, the voltage source is set as follows.
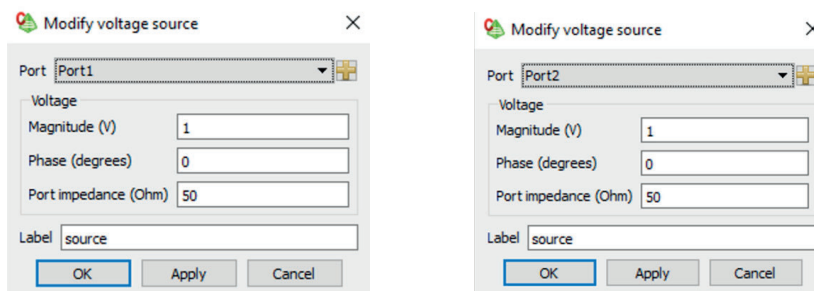
Figure 6.22: Voltage source for both port 1 and port2

Once the solver is run, check for any errors in the simulations. If not, the simulation is said to be complete.

Simulation Results

7.1 Optimization & Simulation Results

Once the simulation is completed, the POSTFEKO option needs to be selected, where the results can be evaluated.

7.1.1 Reflection coefficient

The reflection coefficient graph was obtained as represented below in Figure 7.1.

Excitation
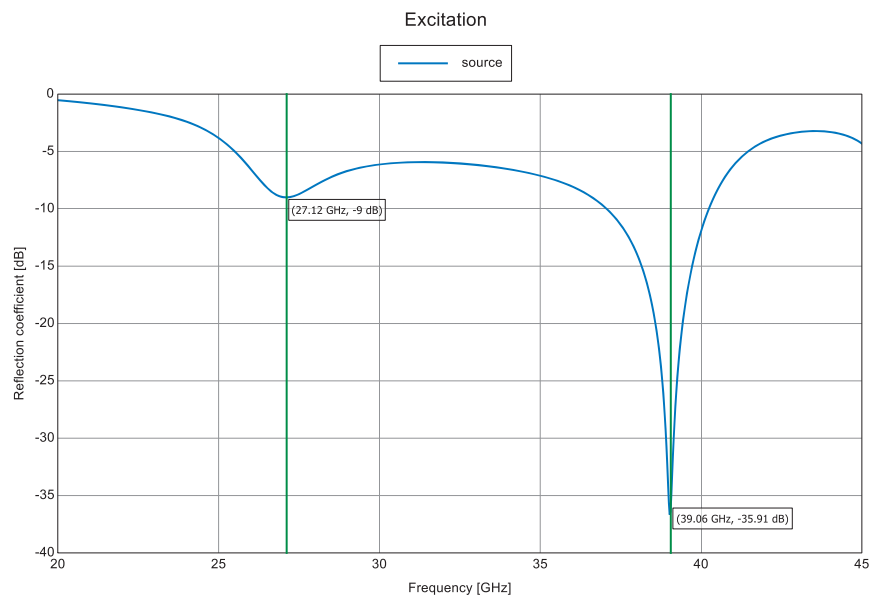
Figure 7.1: Reflection coefficient magnitude plot [dB]

31

It can be observed that the resonant frequencies for the designed antenna model was obtained at around 27.12 GHz and 39.06 GHz, with reflection coefficients of -9dB and -35.91 dB respectively. The reflection bandwidth is measured for both the resonant frequencies as shown in Figure 7.2 below.
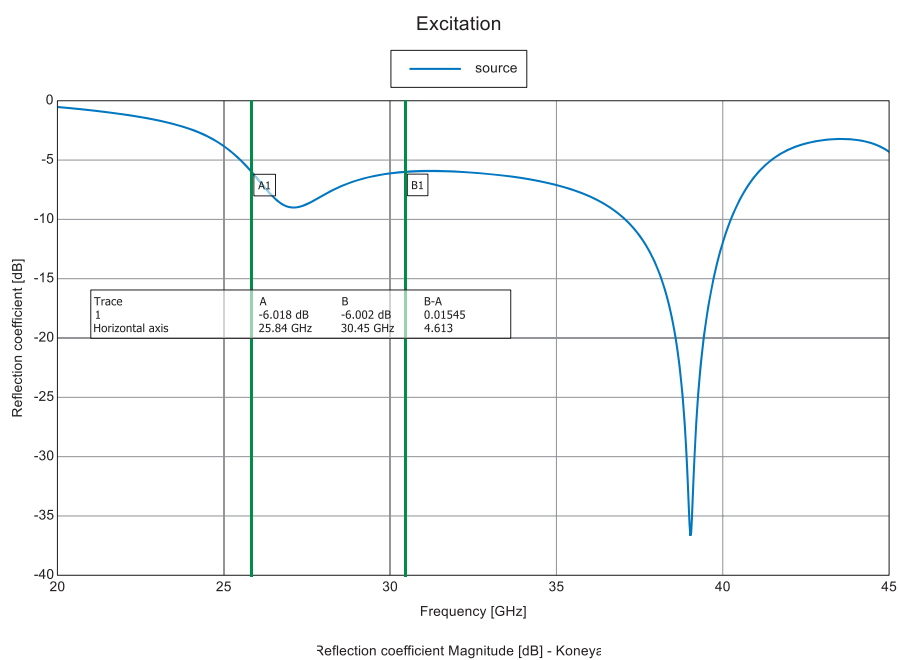
Figure 7.2: Reflection Bandwidth measurement for 28 GHz [dB]

For 28 GHz, the bandwidth obtained is 4.613 GHz with the acceptable return loss as mentioned previously in chapter 4.

Excitation
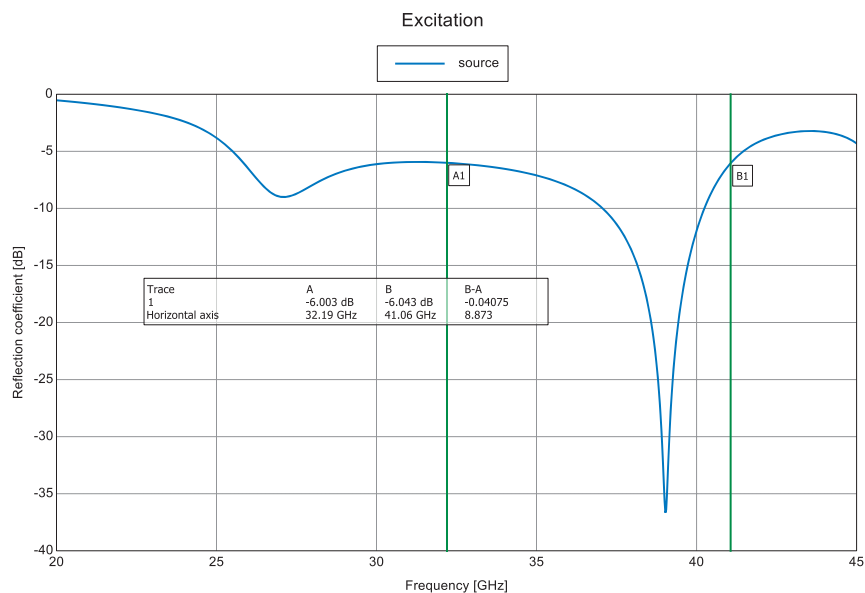
Figure 7.3: Reflection Bandwidth Measurement for 39 GHz [dB]

For 39 GHz, the bandwidth obtained is 8.873 GHz with the acceptable return loss as mentioned previously in chapter 4.

7.1.2 Impedance Matching

A good impedance matching is significant for an antenna design to have as much less mismatch loss that could occur. To indicate the same, the real and imaginary impedances curves were plotted in order to get the impedance matching for both resonant frequencies.

It can be clearly observed from Figure 7.4 below that the real impedances (in blue) are 51.2 Ω and 49.1 Ω obtained for both 28 and 39 GHz, closely match to the input impedance 50 Ω.

Excitation
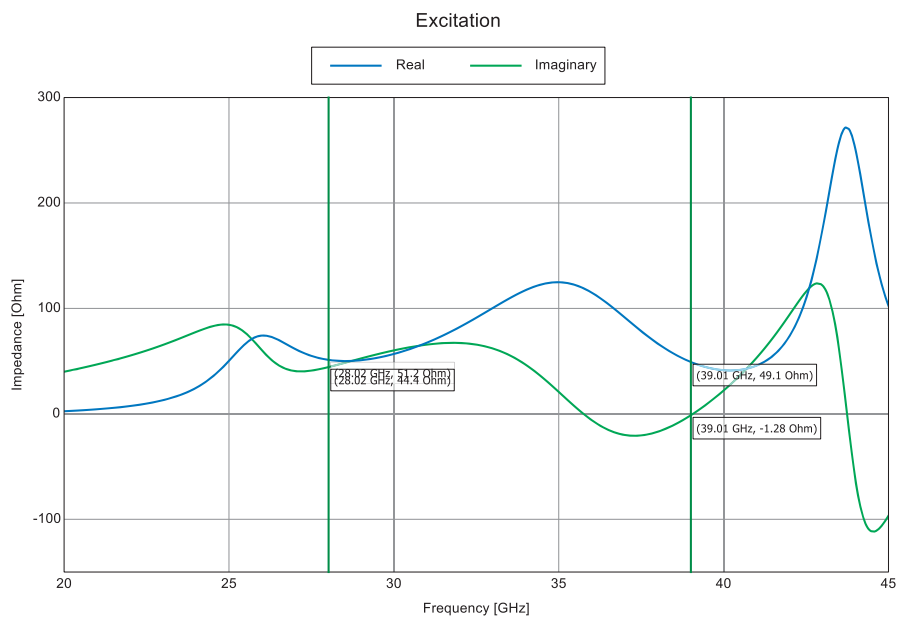
Figure 7.4: Impedance matching plot

7.1.3 Gain & Radiation pattern

The gain value obtained for 28 GHz was about 3.26 dBi as shown in Figure 7.5 below.
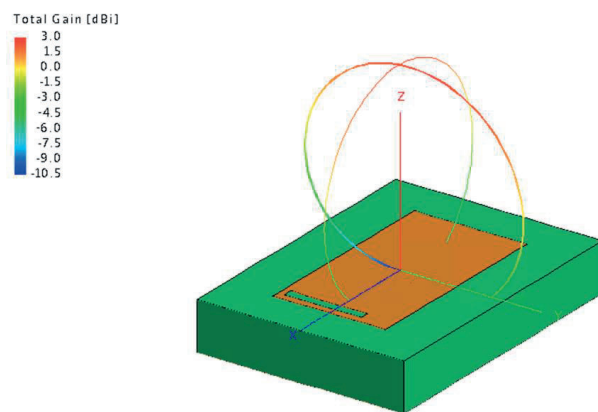
Figure 7.5: Radiation pattern for 28 GHz

Similarly, the gain obtained for 39 GHz was about 1.88 dBi with the radiation pattern looking as shown in Figure 7.6. The shape of the radiation pattern obtained does not typically look like the radiation pattern obtained in Figure 7.5, meaning that there is lesser radiation at say 0 degree but better and higher radiation at 45, 135 degrees. This pattern was carefully assessed by obtaining the gain values for all θ and φ values and analyzing the surface currents.
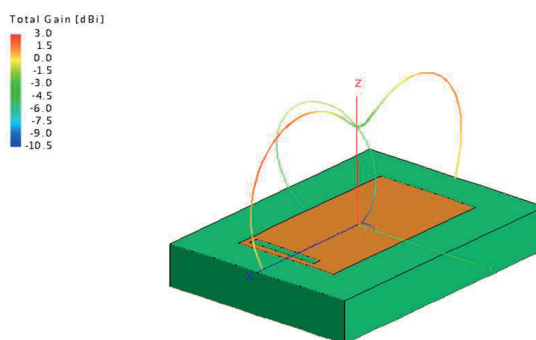
Figure 7.6: Radiation pattern for 39 GHz

7.2 Extracting the simulated results

Since the gain results are required as inputs to the MATLAB code (explained in chapters 8 & 9 ahead), efforts were made to export the CADFEKO data into an excel format. The requirement in the MATLAB code was to get the values of φ from -180 degrees to 180 degrees and θ values from 0 to pi degrees. To perform the same, in the CADFEKO tool, in the *Requests* tab, the following settings were configured.
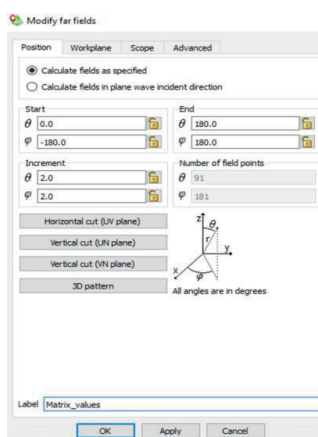
Figure 7.7: Far field values plotted for θ = 0:180 and φ = -180: 180 degrees
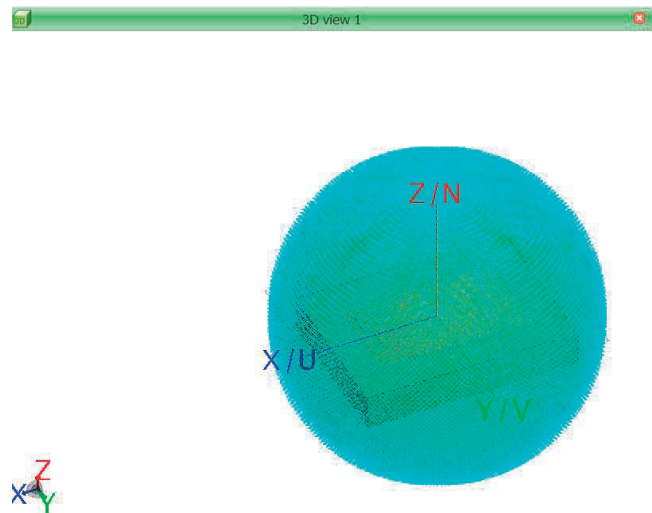
Figure 7.8: Field points for θ and φ represented in 3D model

Figure 7.8 represents 91 field points for θ and 181 field points for φ, with reference to Figure 7.7. Although the defined field points cannot be easily visulalized, they ensure to calculate the gain values for each θ and φ mentioned.

Therefore, we obtained the gain values for all θ and φ values in the form of .ffe format, which was exported from POSTFEKO. Ahead from this point, .ffe format file was converted to an excel format. This excel was directly used in MATLAB, by using the 'Import Data' option.

Beamforming & Link Budget calculations

8.1 Introduction

This chapter mainly covers digital beamforming for handheld devices with relevance to the daily usage of how the cell phones are held and used, simulation performance by placing antennas in distributed placement, accompanied by terminologies explaining how the radiation pattern and transmission performance was achieved by plotting CDF curve.

In a real-life scenario, the way people hold phones while talking, gaming or watching a movie and many more can be different. Therefore, to have a strong hold and an appropriate approach to achieve digital beamforming, we performed a small survey with 5 people on how they hold and use their phones in the given scenarios discussed. This helped us develop 3 widely categorized ways of holding phones which we describe ahead in the chapter as non-blocked cases, blocked (horizontal and vertical) cases.

8.2 Background

Although the 5G mmWave technology has considerable potential, it also poses abundant challenges in both short and long ranged communication. As discussed in Chapter 1, due to the high isotropic path loss in 5G mmWave frequency band, the necessity to have a large number of antenna elements becomes significant. The antenna arrays thereby ensure to help overcome this loss by providing enhanced directional gain through a technique called beamforming [2]. This is employed in 5G NR systems where numerous antenna elements transmit the same signal at an identical phase and wavelength, together generating a single antenna that has a targeted stream formed by reinforcing the waves in a particular direction [7]. In essence, one can affirm that a transmitter-receiver pair may use as many antennas and implement the beamforming technique, with the prime intention to mitigate the high isotropic path loss observed.

Figure 8.1 illustrates how the beamforming technique can be applied in a 5G NR system.
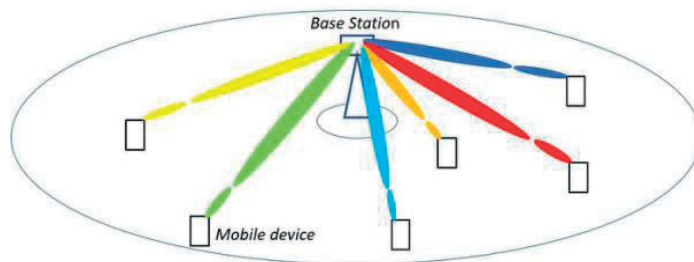
Figure 8.1: Beamforming technique applied in 5G NR system. **Source:** [2]

Here, there is a single radio base station, and 6 mobile devices in a 5G-NR cell (in a real scenario, there would be an arbitrary number of mobile devices). The communication between the radio base station and any mobile device occurs by means of directing the radio signal towards each other using numerous antenna elements at both transceiver ends. The number of antenna elements could range from 64 to 256 in a radio base station and about 4 to 16 in a mobile device for 5G mmWave communication [2].

Beamforming can be incorporated in 3 methods - analog, digital or a combination of both called hybrid. Currently 5G mmWave mobile devices exercise classical analog beamforming [8].

8.3 Analog Beamforming

As represented in Figure 8.2, analog beamforming is performed at the RF through a bank of phase shifters, one per antenna element, an analog power combiner (receiver) and power splitter (transmitter). The radio architecture has one pair of up and down converting mixers accompanied by ADC and DAC at the baseband, both at the transmitter and the receiver [2].
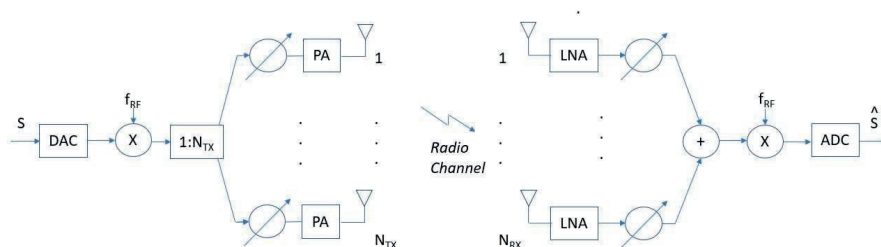
Figure 8.2: Analog Beamforming radio architecture. **Source:** [2]

The description of the analog beamforming radio architecture can be elaborated as follows. To begin with the transmitter side, 'S' represents the transmitted baseband signal which goes through the DAC and gets converted to a radio signal in a single up-converting mixer. This later gets split using a power splitter and fed to a bank of phase shifters mentioned, that are used to perform beamforming. Furthermore, moving to the receiver end, the respective received signal is fed to a phase shifter and later, the beamformed received signals are combined and downconverted in a single mixer to a baseband signal, just before the ADC[2].

This beamforming radio architecture evidently can transmit the radio signal in just one single direction, at a given instance of time. For example, when analog beamforming is used in the case where the mobile device is constantly moving faster relative to the radio base station, the ability to track the radio signal in the direction of transmission as well as quality of service will be degraded, which means low data rate and loss of radio synchronization. Besides, the phase shifters could cause uncertainties leading to a performance loss in stationary cases. These factors therefore limit the possibility of using this beamforming technique, even though it is counted on for its power efficiency[2].

8.4 Digital Beamforming

As a contrasting viewpoint from Section 8.3, the digital beamforming radio architecture is introduced. The beamforming here is performed in the digital baseband processor as shown in Figure 8.3.
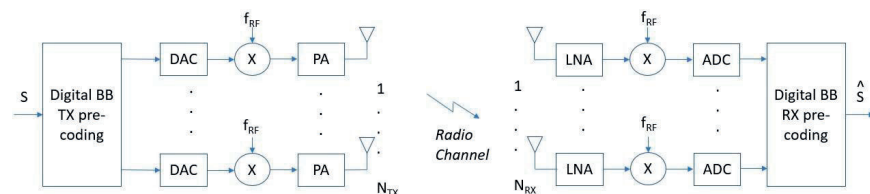
Figure 8.3: Digital Beamforming radio architecture. **Source:** [2]

On the transmitter end, the transmitted signal 'S' is pre-coded/ beamformed for a respective transmitter chain, where each transmitter chain has the DACs and up-converting mixers. Correspondingly, at the receiver end, the beamforming is performed after the ADC, where the receiver chain has a pair of down-converting mixers and the ADCs. Hence, this transceiver chain enables to direct the beams simultaneously in theoretically infinite number of directions at a given instance of time. Thus, digital beamforming radio architectures are preferable over analog beamforming as they have full channel knowledge for all antennas and perform optimal combining after the channel information is obtained, while analog

beamforming first needs to combine, then measure the channel and then update the combining weights. Furthermore, digital beamforming architectures are quite reliable at tracking radio signals when mobile devices are moving faster relative to the radio base station. In addition to this, the pre-coders defined in Figure 8.3 can be achieved in a much easier approach, thereby not compromising on the implementation losses when compared to the analog architecture[2].

In today's evolving market, the mobile devices that support 5G mmWave frequency bands are incorporating the mentioned analog beamforming radio architecture with reference to Figure 8.2. As discussed in Chapter 1, this architecture is quite bulky due to the antenna panels and therefore resulting in a large footprint in the device, as represented in Figure 1.2.

In order to compensate for the disadvantages mentioned and to ensure better benefits with respect to beamforming, digital beamforming radio architecture is implemented. Referencing to Figure 1.2, this architecture comprises an RF chip of size 3×3 mm^2 with a total footprint coming up to 144 mm^2 , which is relatively less bulkier compared   to   the   analog   beamforming   radio   architecture.

The usage of analog beamforming radio architecture can be entailed more with a daily life example. Assume that a user holds the mobile device in a certain way that some or most of the antennas are covered. This results in the blocking of the radio signals by the hand of the user. Although there are 64 antenna elements placed (As represented in Figure 1.2)., there could be approximately 8 to 16 of them being active and radiating due to the blocking mentioned. In this thesis, the distribution of the antenna elements for analog beamforming scenario is assumed to be arranged as linearly close spaced arrays (as explained ahead in Figure 9.21) and the digital beamforming scenario assumes singular antenna distributed on a larger surface (of the mobile device).

Therefore, it can be asserted that the current mobile devices may have sufficient UL TX power in an ideal and unobstructed non-block case, unlike the non-ideal or blocked case.

8.5 Link budget calculations and EIRP TX requirements

To elaborate more on the non-ideal or blocked case, one can consider performing the link budget calculations as Figure 8.4 below.

		Data channel	
		Uplink	Downlink
Total BW		200MHz (100x2)	400MHz (100x4)
MCS		QPSK	QPSK
PRBs per CC		66	66
Throughput (Mbps)		5	50
Transmitter			
100% min EIRP		22.4	60
50% min EIRP		11.5	
Receiver			
Thermal Noise Density (dBm/Hz)		-174	-174
Receiver Noise Figure (dB)		6	10
Occupied Channel BW (MHz)		95.04	95.04
Effective Noise power		-88.22093572	-84.22093572
Required SINR		-0.9	-3
Rx BF Gain (dBi)		29	8
Implementation Margin (dB)		0	0
Receiver Sensitivity		-118.1209357	-95.22093572
MCL (with 100% min EIRP)		137.5106358	149.2003358
MCL (with 50% min EIRP)		126.6106358	

Table 7-1 28GHz Link Budget

Figure 8.4: An example for Link Budget calculations for 28 GHz **Source:** [14]

It is observed that, at 50% minimum peak EIRP at the TX, the typical value obtained is 11.5 dBm, that is about 51.34% of power loss. The 50% minimum peak EIRP is the median value and becomes a focal point of interest in the link budget because this deteriorated value is obtained due to the blocking of antennas as a result of holding the mobile device in unfavorable positions. A detailed explanation about the type of holding is explained in Section 9.5. Consequently, the beams are not aligned perfectly with the direction to the base station. Minimum peak EIRP is defined as the lower limit without tolerance, where the test tolerances are used to relax the minimum requirements in this specification to create test requirements [15]. Hence, it can be stated that UL is the limiting factor in the current 5G mmWave deployment. Efforts are made to compensate for this EIRP TX loss in the uplink by incorporating a digital beamforming approach called the distributed antenna element approach, as shown in Figure 8.5.

Front
Back
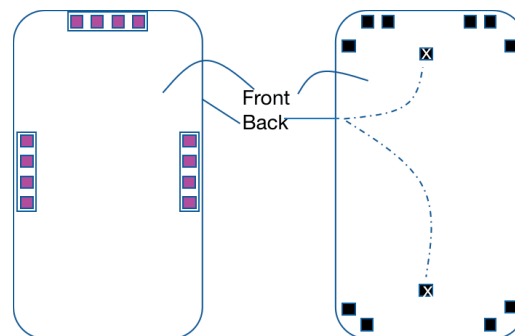
Figure 8.5: A comparison between placement of antennas in analog beamforming & digital beamforming

The EIRP at the TX for both the frequencies (28 GHz and 39 GHz) are evaluated based on link budget calculations assumptions above and under the following further assumptions about the transceiver output power, antenna gain etc.

Frequency 1: 28 GHz

- Maximum PA output power: 14 dBm
- Front end loss: 1.5 dB (Switch 26/39GHz PAs + feed loss is considered)
- Maximum active PAs: 4
  - Power gain: 6 dB
  - Beamforming gain: 6 dB

- Antenna gain: 3.26 dBi

The antenna gain value for 28 GHz mentioned above is obtained from our designed patch antenna (explained in Chapter 4) and is extracted as a result of all far field points defined for desired θ and φ values, discussed in Chapter 7.

Therefore, the maximum EIRP TX power for 28 GHz: 14-1.5+6+6+3.26 = 27.76dBm.

Frequency 2: 39 GHz

- Maximum PA output power: 14 dBm
- Front end loss: 1.5 dB (Switch 26/39 GHz PAs + feed loss is considered)
- Maximum active PAs: 4
  - Power gain: 6 dB
  - Beamforming gain: 6 dB
- Antenna gain: 1.88 dBi

The antenna gain value for 39 GHz mentioned above is obtained from our designed patch antenna (explained in Chapter 4) and is extracted as a result of all far field points defined for desired θ and φ values, discussed in Chapter 7.

Therefore, the maximum EIRP TX power for 28 GHz: 14-1.5+6+6+1.88= 26.38dBm.

8.6 3GPP Technical specifications

With reference to Figure 8.4, the link budget calculations are performed according to the 3GPP Technical Specification 38.101-2, Section 6.2.1.3 [15] for 5G NR UE radio transmission and reception. For a handheld mobile device or UE categorized as power class 3, the minimum peak EIRP in the direction of the beam ranges from 20.6 to 22.4 dBm, depending on the NR band. The below describes the mentioned specifications.

Operating band	Min peak EIRP (dBm)
n257	22.4
n258	22.4
n260	20.6
n261	22.4

Table 1: UE minimum peak EIRP for power class 3

Besides, the minimum peak EIRP at the 50th percentile of the CDF distribution of radiated power measured over the full sphere around the UE is defined as the spherical coverage requirement [15] that is a lower limit without tolerance. This is represented in the below table.

Operating band	Min EIRP at 50th %-tile CDF (dBm)
n257	11.5
n258	11.5
n260	8
n261	11.5

Table 2: Minimum EIRP at 50th percentile CDF

It is to be noted that these specifications and requirements are defined assuming analog beamforming (as shown in the tables 1 and 2) in the antenna panel direction, accompanied by a minimum peak EIRP requirement of 50% coverage, where the antenna panel is not pointing in a favorable direction relative to the base station.

Based on these data, we set our internal requirements for a distributed antenna placement approach, as follows.

EIRP requirement	EIRP Tx power in dBm
Minimum power requirement (in any direction or specific beam direction)- NonBlock	23
Minimum peak EIRP requirement (at 50%) in 90% of the sphere- Block	12

Table 3: Internal EIRP Requirements

Binding to these requirements and yet using as few antennas as possible, considering cost and power constraints, were quite a challenging task to implement. Further details about this approach are entailed in Chapter 9.

MATLAB Simulation results

9.1 Introduction

This chapter starts with elucidating the import of the extracted far field points for all θ, ɸ from Altair FEKO to Excel, as discussed in Chapter 7, Section 7.2. From the extracted data, only the total gain values have been consolidated. These consist of all the gain values in both θ, ɸ directions which are then formulated into a matrix format and later uploaded to the MATLAB based software, in order to view the gain and radiation pattern by using the digital beamforming or distributed antenna element approach, mentioned in Chapter 8. Besides, in this chapter, the major comparison between analog and digital beamforming is shown for 5G mmWave FR2 frequencies. Finally, the CDF for EIRP TX power is plotted by assuming random direction of transmission for both analog and digital design scenarios and for different hand blocking scenarios.

9.2 Extracting Gain values from Altair FEKO to MATLAB

As explained in Chapter 7, the far field points for all θ, ɸ were calculated using the 3D coordinate systems. By definition, the coordinate system is a system that uses one or more number of coordinates to uniquely determine the location of the points in space. Here, the Altair FEKO has used spherical coordinate system to identify the far field points.

The spherical coordinates often use two orthogonal directions the zenith and azimuth reference, and an original point on the space. This is shown in Figure 9.1. The figure also contains the globe showing the radial distance 'r', the inclination angle ɸ, and the azimuthal angle θ. The radius or the radial distance is the Euclidean distance from origin O to P. The inclination or the polar angle between the zenith direction and the line segment OP and the inclination angle ɸ vary between -180 to 180 degrees.

The θ is the signed angle measured from the azimuth reference direction to the orthogonal projection of the line segment OP on the reference plane and the azimuthal angle θ vary between 0 to 180 degrees [16].
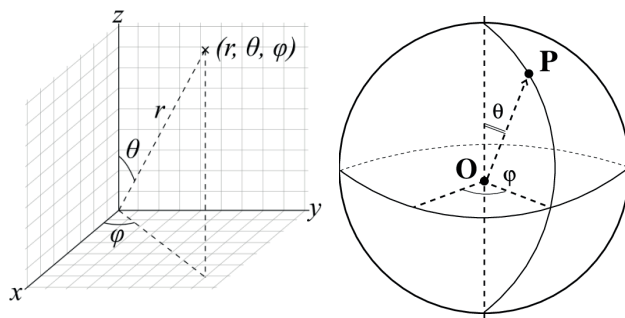
Figure 9.1: Spherical coordinate system

The steps for far field points in the θ, φ directions were incremented by 2, as shown in Figure 7.7. Therefore, the total number of far field points are θ=91 and φ=181. The total gain values for all field points were imported and consolidated in an excel to form a matrix of size 16471 x 3, where the columns of matrix are φ, θ and total gain respectively. As mentioned in Chapter 7, the total gain values obtained were in. ffe format and therefore converting from .ffe to excel was required, and all the values were in scientific format. As we may know, using this scientific format directly into MATLAB for processing data may be complex to resolve, hence conversion to number format was performed so that it can easily be implemented in the MATLAB code. With the utilization of total gain values in this MATLAB code, further analyses are done with the help of MATLAB based simulator entailed in the next subsection.

9.3 MATLAB based simulator: 'Device antenna radiation visualizer'

The main objective for using this MATLAB application is to visualize how the radiation and the gain patterns which describe the EIRP TX power (in dBm) obtained based on the placement and blocking of active antennas, performed by using virtual mobile test. The virtual mobile test is conducted by placing the antenna on the mobile phone and by computing radiation pattern along with the mobile phone assuming both analog beamforming with antenna panels and digital beamforming/distributed way.

There are 3 different features in the MATLAB application, they are transceiver parameters, commands and mobile parameters as explained in Figure 9.2.

9.3.1 TRANSCEIVER PARAMETERS

As shown in Figure 9.2, the antenna parameters consist of number of RF chip, active RF chip, blocked RF chip, blocking factor in dBm, reference RF chip, minimum power amplifier output power in dBm, power amplifier output power in dBm, total number of paths and power profile for the paths. All these parameters impact the simulation and only meant for user interaction.

#RF chip - The number of antenna elements that the user wants to be deployed on the phone.

#Active RF chip - The number of used antenna elements for beamforming.

#Blocked RF chip - The number of antenna elements that the user assumes to be blocked (by the hand) on the phone.

Blocking factor [dBm] - Signal loss in dB in each blocked antenna element.

#Reference RF chip - The number of antenna elements that are used as reference in in the plots, should be the same as #Active RF chip if the user does not specifically wish to examine differences based on the number of active antennas.

Min PA o/p power[dBm] - The minimum output power in dBm used in the color bar, the
maximum PA output power is determined by the #Reference RF chips.

PA o/p power[dBm] – power amplifier's output power into the antenna.

#Paths - The number of active paths, only used when choosing signal direction manually. In this study, we only looked at radiation plots assuming one radio path (LoS).

Power profile path# - Used when #Paths ≥ 2 to determine the path power profile (in dBm).

Plot nbr (name) - The only parameters that does not affect the simulation, determines the number of the plot, hence the user should change the number after each plot in order to not overwrite previous results.

9.3.2 COMMAND FEATURES

As shown in Figure 9.2, the command feature consists of load necessary function, place antennas, block antennas, show radiation patterns, choose signal direction 2D, choose signal direction 3D and use manual coordinates.

Load necessary function – It is important to press this load necessary function, when the MATLAB application is started because it will execute a few requisite processes

to generate antenna gain in all 6 directions in XYZ plane based on the reference antenna used which radiation pattern is defined for a patch antenna in the XY-plane.

Place antennas - This button will load a window that lets the user see a 2D sketch of the 6 different sides (front, back, left side, right side, top side, bottom side) of a mobile phone. The user will be able to distribute the same amount of antenna element as the value of #RF chip by clicking on the different sides of the phone.

Block antennas - This button will deploy the antenna elements and allow the user to block the antennas. The number of antennas the user will block is determined by the #Blocked RF chip parameter. When an antenna is blocked it turns red to let the user know that it has been blocked which means the signal into the antenna element is suppressed with #Blocking factor dBm mentioned in 9.3.1.

Show radiation pattern - This button calculates the Total o/p power in each direction and showcases it as a spherical plot. Conjectures are done in such a way that we assume ideal outgoing signal for every angle of approach in a sphere around the mobile phone. This implies that the result will be a spherical plot with its color representing the EIRP TX power in [dBm] at that specific angle of approach. The parameter Min Total o/p power [dBm] will work as a scalar for the colorbar that sets the color variation from blue = min Total o/p power, to red = max PA o/p power.

Use manual coordinates - This button has the same purpose as" Choose signal direction" to let the user see which antennas are active for a certain angle of approach.

9.3.3 MOBILE PARAMETERS

As shown in Figure 9.2, the only assumption done is that the base station is fixed in the origin so the coordinates of the mobile phone changes with respect to the origin (base station).

For example if the user gives the coordinates (5,3,-2) it means that the position of the mobile phone is 5 meters east, 3 meters north and 2 meters below the base station. Because we assume that all the incoming signals are parallel (Fraunhofer region) the unit of length for the coordinates does not matter i.e, the coordinates (1, 1, 1) gives the same result as (10, 10, 10).

• X - Positive: east, negative: west

• Y – Positive: north, negative: south

• Z - Positive: Above, negative: below

• α - Positive direction: Clockwise

- β - Positive direction: Turning left

- γ – Positive direction: Diving

The rotations have negative orientation and thus following the inverse of the right-hand rule for each axis.

With regards to the MATLAB simulator mention in this section, no investigations or studies were performed by us in this study.

9.4 MATLAB Application

STEP1 - As the first step, it is required to run the MATLAB script which generates the application window shown in Figure 9.2 below.

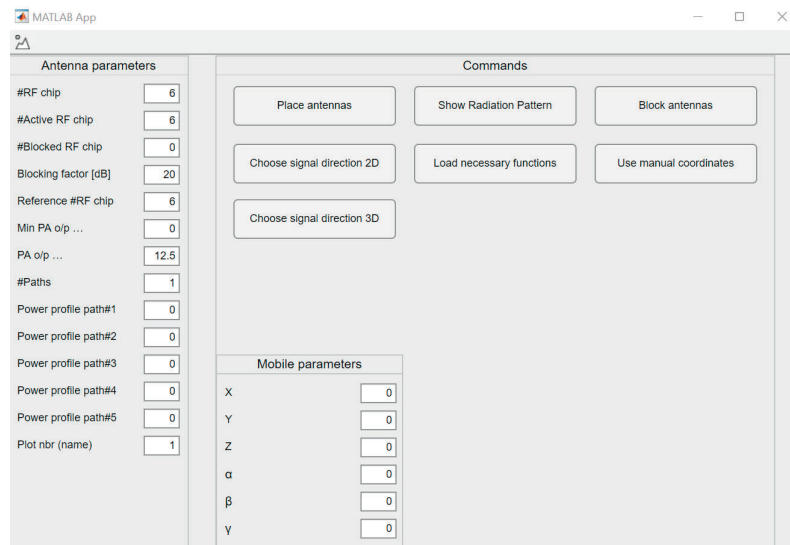**Figure 9.2:** MATLAB Simulator application to place & block antennas and obtain spherical radiation pattern

As soon as the application window is popped, need to press the 'Load necessary function' button so that the antenna parameters on the left side are enabled to change.

In the above Figure 9.2, as an example 6 antenna elements are distributed. Therefore, both #Active RF chip as well as Reference #RF chip are set to 6.

STEP2 –Post Step 1, the 'Place antennas' button needs to be pressed. This feature will help to place the antennas according to the requirement. Figure 9.3 shows all the 6 different sides of the mobile phone in 2D view.
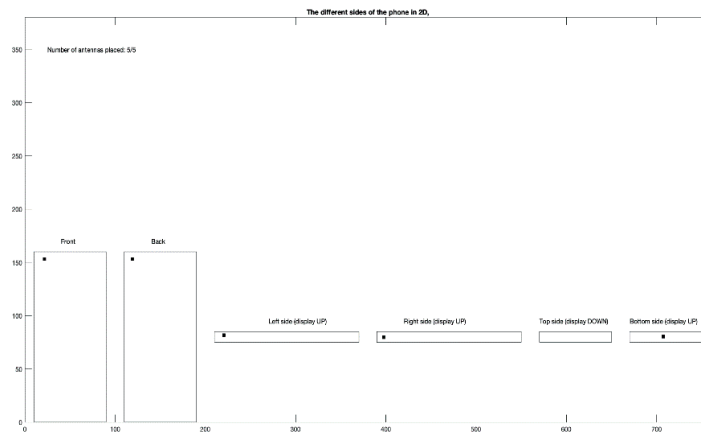
Figure 9.3: Distributed Antenna Placement approach

After distributing the antenna elements, ensure not to close the window, but to minimize it, in order to use it for blocking the antenna elements whenever required.

STEP 3 – In this step, the pattern will be displayed by pressing 'Show radiation pattern'. This pattern represents the sum, in power, of all the different antennas coverage and therefore the simulator illustrates the overall coverage due to antenna elements. One can choose to drag and change the rotation of the plot by left clicking it. The short (or bottom) side of the mobile phone is aligned with the x-axis, the long (or left) side is aligned with the y-axis and the (front panel) is align with the z-axis.
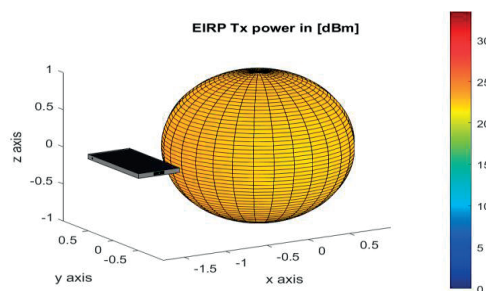
Figure 9.4: Display of the radiation pattern

From Figure 9.4, it can be noticed that there is a small black rectangle on the 3D model of the mobile phone. It is used to symbolize the charger port, which means that it is the bottom side of the phone. The placed antenna elements are highlighted in green, blocked ones will be highlighted in orange, which are elaborated in detail in Section 9.5 ahead in this chapter.

STEP 4 – After placing the antenna, based on the different hand holding scenarios where the hand may block some of the antennas degrading the radiation pattern in some directions. For example, 3 blocked antennas are shown and the corresponding radiation pattern is obtained, which are represented in Figures 9.5 and 9.6.

Figure 9.5: Blocking of few of the antennas (in red) based on the user's way of hand holding the mobile device
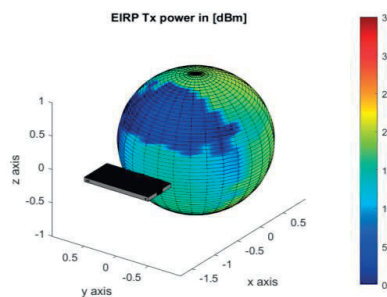
Figure 9.6: Radiation pattern obtained based on the number of blocked antennas and therefore indicating their coverage patterns

9.5 Implementation of sub array based analog beamforming and distributed antenna element approach based digital beamforming

There is always a need to receive signals equally from all directions to have a better coverage around the mobile phone. In order to get such an omni directional coverage, the placement of antenna pla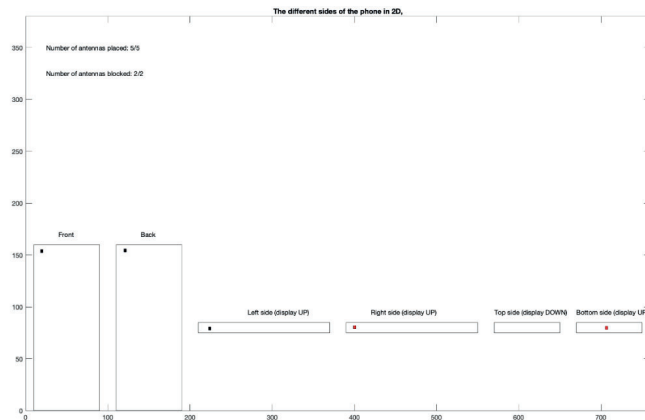ys a crucial role. Hence to have an isotropic coverage, the antenna elements have been distributed in different places on the mobile phone.

9.5.1 Type of holding the mobile phone

A small survey was conducted among 5 people to analyze how they hold the phone in different scenarios like texting, watching, playing game.

Vertical holding – This type of holding will block antennas placed on the left, right and bottom part of the phone.

Figure 9.7: A typical way of holding the mobile device vertically by a user for example, while texting or writing email etc.,

Horizontal holding – The type of holding represented on the left in Figure 9.8, will considerably block antennas placed at the top, bottom and left /right part of the phone. Similarly, the type of holding represented on the right in Figure 9.8, it is possible to block antennas on the back side of the phone sometimes. It majorly depends on how people hold the mobile phone yet shown as a typical example.
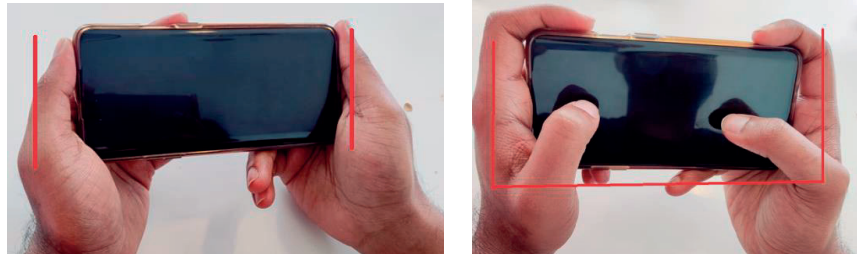
Figure 9.8: A typical way of holding the mobile device horizontally by a user. For example, while playing games or watching a movie etc.,

9.5.2 Placements of antenna elements

As stated in Chapter 4, the antennas used for placements in this chapter is designed to resonate at 28GHz and 39GHz. In this section, simulation experiments and results have been extracted for both analog and digital beamforming to understand the behaviours for both assuming using the antenna designed. Therefore, for 28 GHz, the total number of antennas used for digital beamforming are 5 and for analog beamforming, 6 are used. Similarly, for 39GHz, a total of 6 antenna elements were used for both analog and digital beamforming.

The above-mentioned number of antenna elements are decided as the lower bound requirement in order to obtain an acceptable omnidirectional coverage, thereby satisfying the internal requirements defined in Table 3, Section 8.5.

In all the subsection mentioned below, ▣ represents the active antenna on the back side, ▣ represents the active antenna on the front panel, ▣ represents the blocked antenna element and ▣ represents the active antenna element placed on either left, right, bottom or top sides of the mobile device.

- Distributed antenna element approach for digital beamforming – Non-Block case at 28GHz

Figure 9.9: Non-block case - 28 GHz: A mobile device represented with 5 active antennas

Here, total number of antenna elements used are 5 and their placements are one in the antenna in the front panel (placed in the corner), one on the back (placed in the corner), one on the left top corner, one on the right bottom corner and last one on the bottom side (placed in the middle).

Figure 9.10 shows the 3D coverage for digital beamforming non-blocking case at 28GHz, and it is seen that EIRP TX power is above 23dBm in any direction. It is to be mentioned that the plot in below figure shows EIRP TX power in respective direction which is obtained because the transmitted signal is assumed to be perfectly phase shifted from each transmitter antenna for each direction of the sphere. Therefore, this explanation applies to all the EIRP TX power radiation patterns expressed in this subsection, where the radiation fields are explained in far field (as discussed in Chapter 3).

Figure 9.10: Non-block case - 28 GHz: Spherical coverage representing the total EIRP TX power

- Distributed antenna element approach for digital beamforming –
  Vertical block case at 28GHz

Figure 9.11: Blocked case (Vertical) - 28 GHz: A mobile device with 1 antenna placed at the front panel, 1 at the back panel, 1 on the left-side are active, while the antenna placed on the right-side and 1 at the bottom side are blocked

As represented in Figure 9.11, the total number of antenna elements used are 5. Due to vertical holding case, the antenna elements placed at the bottom and the right bottom will be blocked. Figure 9.12 shows the 3D radiation pattern for digital beamforming vertical blocking case at 28GHz, and it is seen that EIRP TX power is clearly above 12dBm in any direction. The EIRP TX power target is in accordance with 3GPP, i.e., 12 dBm, also for the blocked case in above 90% of the sphere, as stated in Chapter 8.

Figure 9.12: Blocked case (Vertical) – 28 GHz: Spherical coverage representing the total EIRP TX power

- Distributed antenna element approach for digital beamforming –
  Horizontal block case at 28GHz

Figure 9.13: Blocked case (Horizontal) – 28 GHz: A mobile device with 1 antenna placed at the back panel and on the right side are active, while the antenna placed at the front panel, 1 on the left-side and 1 at the bottom side are blocked

As per Figure 9.13, the total number of antenna elements used are 5. Due to horizontal holding case, the antenna elements placed at the left corner, bottom middle and the front will be blocked.

Figure 9.14 displays the 3D radiation pattern for digital beamforming horizontal blocking case at 28GHz, and it is seen that EIRP transmit power is above 12dBm in more than 90% of the directions.

Comparing figures 9.12 and 9.14, one can interpret that the EIRP TX power in Figure 9.12 is better because 2 antennas are blocked. In Figure 9.14, 3 antennas are blocked and therefore the EIRP TX power is relatively lower.

It is to be noted that both blocking scenarios have nearly the same low EIRP TX power as fewer antennas are placed in bottom side of the mobile phone and they were blocked.
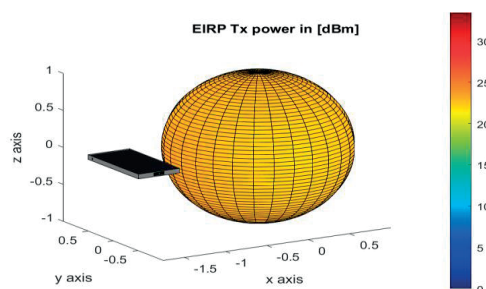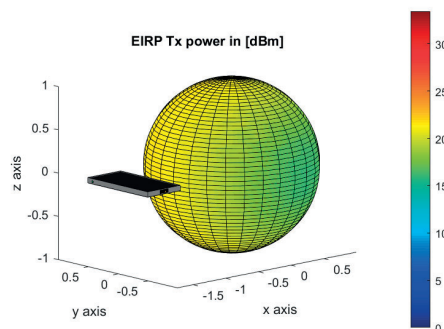

Figure 9.14: Blocked case (Horizontal) - 28 GHz: Spherical coverage representing the total EIRP TX power

- Distributed antenna element approach for digital beamforming –
  Non-Block case at 39GHz

As shown in Figure 9.15 below, the total number of antenna elements used are 6 and their placements are 2 at left side, 2 on top side, 1 at right side and 1 at the back.

Figure 9.15: Non-block case - 39 GHz: A mobile device represented with 6 active antennas

The below Figure 9.16 shows the 3D radiation pattern for digital beamforming non-blocking case at 39GHz, and it is seen that EIRP transmit power is above 23dBm in most of the directions. From the section 8.6, we know that min peak EIRP is 20.6dBm only for beam directions and digital beamforming with distributed architecture can achieve the requirements for almost all directions.

Figure 9.16: Non-block case - 39 GHz: Spherical coverage representing the total EIRP TX power

- Distributed antenna element approach for digital beamforming –
  Vertical block case at 39GHz

Figure 9.17: Blocked case (Vertical) - 39 GHz: A mobile device with 2 active antennas placed on the top side, 1 active antenna at the back panel, 1 active antenna on the right side, 1 active on the left-side (up) and 1 blocked antenna on the left-side (down)

From Figure 9.17, the total number of antenna elements used are 6. Due to vertical holding case the antenna elements placed at the left bottom will be blocked.

The below figure shows the 3D radiation pattern for digital beamforming vertical blocking case at 39GHz, and it is seen that EIRP transmit power is above 12dBm in more than 90% of the directions.
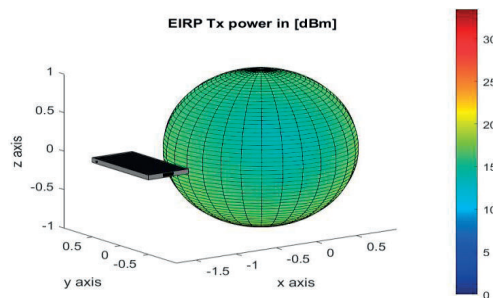

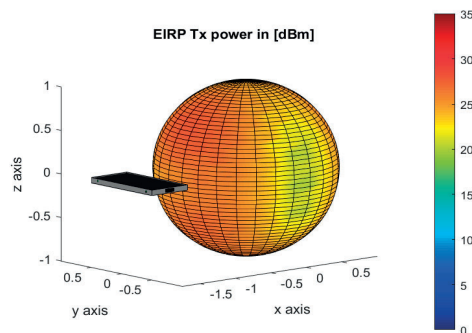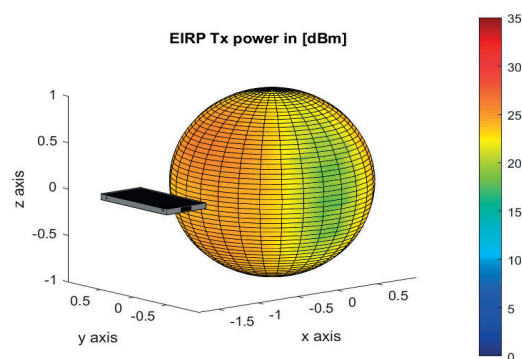**Figure 9.18:** Blocked case (Vertical) - 39 GHz: Spherical coverage representing the total EIRP TX power

- Distributed antenna element approach for digital beamforming −
  Horizontal block case at 39GHz

This scenario is represented in Figure 9.19 shown below, where the total number of antenna elements used are 6. Due to horizontal holding case, the antenna elements placed at the left side, back side and the top left corner will be blocked. Only 2 antenna elements placed at right side and top right corner is active.

Figure 9.19: Blocked case (Horizontal) - 39 GHz: A mobile device with 1 active antenna on the right side, 1 active antenna on the top side, while the antenna placed at the back side, 2 antennas on the left side and 1 antenna on the top side are blocked

The below figure shows the 3D radiation pattern for digital beamforming horizontal blocking case at 39GHz, and it is seen that EIRP transmit power is still above our internal requirement of 12dBm in most the directions.

It is also noted that the performance is not same for both (-90º) and (+90º) because the antenna elements is not same from either side. The total number of antennas that's blocked can be different in other case. Here, (-90º) and (+90º) means type of placement, where the mobile phone is held other way around by blocking 3 antennas.
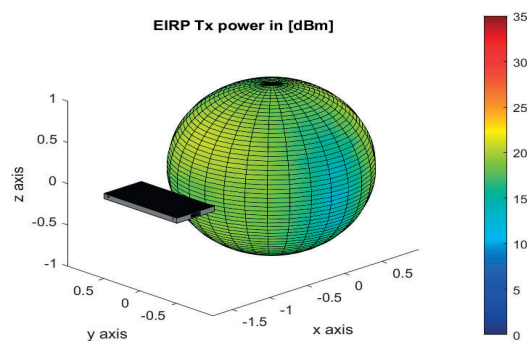
Figure 9.20: Blocked case (Horizontal) - 39GHz: Spherical coverage representing the total EIRP TX power

- Sub array based analog Beamforming - Non-Block case
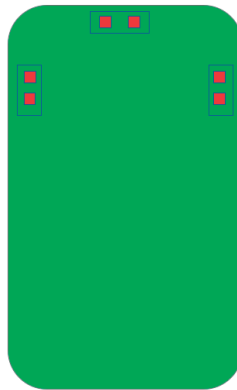
Figure 9.21: Non-block case - 28 GHz and 39 GHz: A mobile device represented with 6 active antennas but in a cluttered manner unlike the distributed antenna placement

The total number of antenna elements used in 3 panels are 6, as seen in Figure 9.21, with each consisting of 1x2 antenna array.

The below Figure 9.22 shows the 3D radiation pattern for analog beamforming non-blocking case for both 28GHz and 39GHz. It is seen that EIRP transmit power is **not** above 23dBm in all the directions, this is still agreeable as per 3GPP specifications explained in Chapter 8, because 22.4dBm EIRP TX power if achieved in at least 1 direction and a minimum of 12.5dBm in 90% of the sphere is acceptable.

Figure 9.22: Non-block case - 28 GHz and 39GHz respectively: Spherical coverage patterns representing the total EIRP TX power

- Sub array based analog Beamforming – Vertical block case
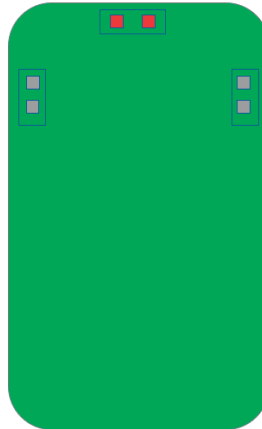
Figure 9.23: Blocked case (Vertical) - 28 GHz and 39 GHz: A mobile device with 2 active antennas placed on the top side while both pairs of antennas on left and right sides are blocked

The total number of antenna elements used in 3 panels are 6 with each consist of 1X2 antenna array. Due to vertical holding case the antenna panels placed at both the left and right will be blocked. Therefore, only one antenna panel at the top is active.

Figure 9.23 shown below represents the 3D radiation pattern for analog beamforming blocking vertical case for both 28GHz and 39GHz. It is seen that EIRP transmit power is **not** above 12dBm in all the directions.

Figure 9.24: Blocked case (Vertical) - 28 GHz and 39GHz respectively: Spherical coverage patterns representing the total EIRP TX power

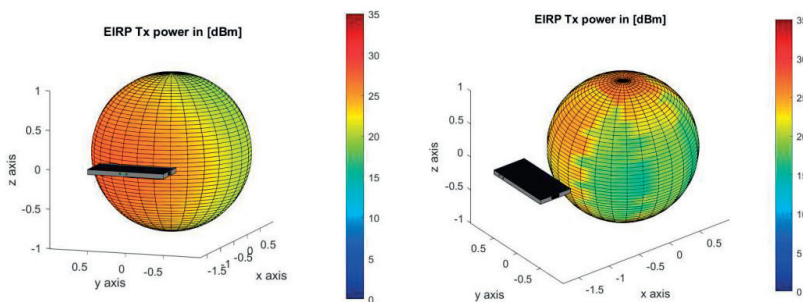- Sub array based analog Beamforming – Horizontal block case
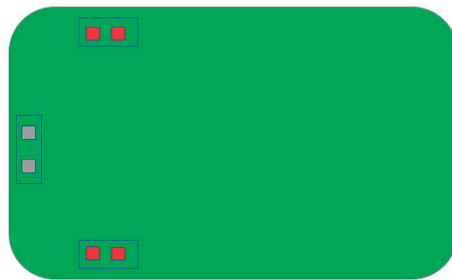
Figure 9.25: Blocked case (Horizontal) – 28 GHz and 39 GHz: A mobile device with 2 pairs of active antennas on the left and right sides while the 2 antennas on the top are blocked

The total number of antenna elements used in 3 panels is 6 with each consist of 1X2 antenna array. Due to horizontal holding case the antenna panels placed at top and the left panel will be blocked. Therefore, only the right antenna panel will be active.

Figure 9.26 show the 3D radiation pattern for analog beamforming blocking horizontal case for both 28GHz and 39GHz. It is seen that EIRP transmit power is not above 12dBm in all the directions.

It is also noted that the performance is same for both (-90°) and (+90°) because the antenna panel is symmetric from either side.
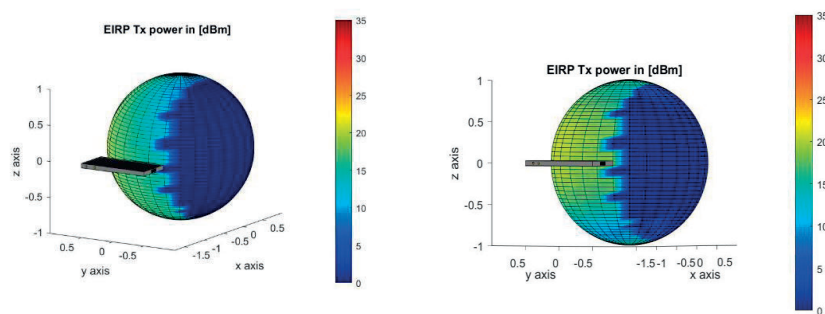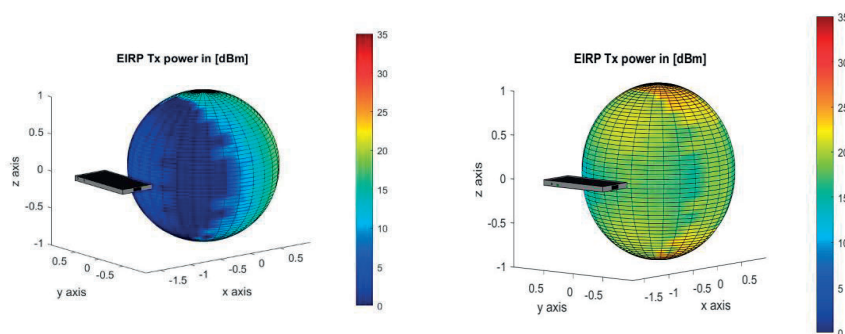

Figure 9.26: Blocked case (Horizontal) - 28 GHz and 39GHz respectively: Spherical coverage patterns representing the total EIRP TX power

9.6 Simulated TX performance for sub array based analog and distributed antenna element approach for digital beamforming

In this subsection, the CDF plot for EIRP TX power is determined by assuming random direction of transmission, where for each direction and for each design the best antenna panels were chosen in analog beamforming and the best 3-4 antennas elements were chosen in digital beamforming.

9.6.1 CDF plots for 28GHz – sub array based analog non-block and block case
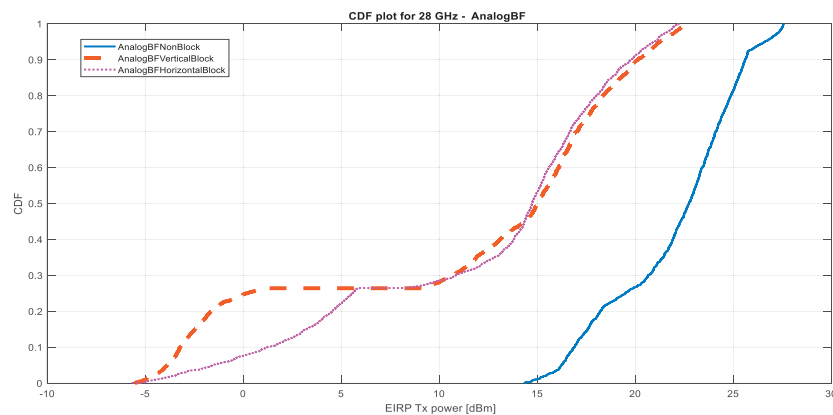
Figure 9.27: CDF plot for 28 GHz –analog beamforming

From Figure 9.27, it can be derived that the EIRP TX power is relatively higher and better for non-block case compared to the block case. In the non-block case, all the 3 panel with 1x2 antenna elements are active and the EIRP TX power is in 75% of the cases above the requirement level. By comparing the two block cases (vertical and horizontal) it is noticeable that almost 70% of the time analog beamforming in horizontal case is better than vertical case, because no antenna panel is placed at the bottom of the mobile phone in vertical case, whereas in horizontal, only one antenna panel is blocked and will receive some signal power from the bottom. There will be roughly about 35% losses in horizontal case compared to vertical case from top side of the mobile phone. Altogether, 40% of the time the worst-case losses are more, which means it leads to much smaller coverage and in worst case call drops.

9.6.2 CDF plots for 28GHz – Distributed antenna element approach for digital
        beamforming- non-blocking and blocking case

Figure 9.28: CDF plot for 28 GHz - digital beamforming

From Figure 9.28, we understood that the EIRP Tx power is high for non-block case
compared to the block case. In the non-block case, all the 5 antenna elements were
active and distributed on the mobile phone unlike analog case. Whereas in blocking
cases, vertical holding is better than horizontal holding because in vertical case the
total number of block antenna is 2 and it is less compared to horizontal case with 3
blocked antenna elements. As observed, the EIRP Tx power is above 12dBm in 95%
of cases in all situations.

9.6.3 CDF plots for 28GHz – Distributed antenna element approach for digital beamforming non-blocking and analog non-blocking case
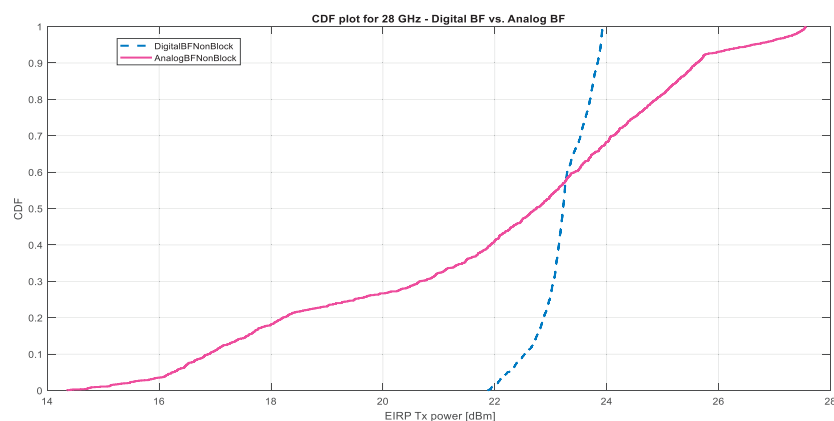
Figure 9.29: CDF plot for 28 GHz - Comparison between analog and digital BF (Non-Block)

Seen from the above plot in Figure 9.29 that, even though we use 6 antennas with 3 panels in analog beamforming, the EIRP TX power is 55% less in some cases compared with 5 antenna elements in digital beamforming. For instance, if we use 6 antenna elements for digital beamforming there will be a fair comparison between the analog and digital beamforming. The digital beamforming will be better in all the cases, but one need to think about the antenna/RF chip power consumption level, cost and size requirements.

In summary, below conclusion can be derived for non-blocking cases. The EIRP TX power at 10% CDF for analog and digital beamforming obtained are 20.9dBm and 22.5dBm respectively. Similarly, the EIRP TX power at 50% CDF for analog and digital beamforming obtained are 23.8dBm and 23.2dBm respectively. These CDF values are acceptable as they satisfy the 3GPP specifications.

EIRP TX power is calculated at (CDF 10% / CDF 50%)

- Sub array based Analog beamforming (non-blocking) – 16.8dBm / 22.8dBm (EIRP)
- Digital beamforming (non-blocking) – 22.5dBm / 23.2dBm (EIRP)

9.6.4 CDF plots for 28GHz –Comparing all the sub array based analog and
distributed antenna element approach for digital cases
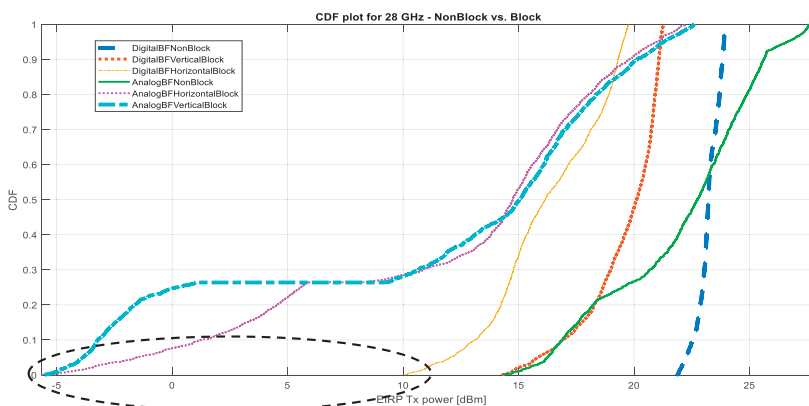
Figure 9.30: CDF plot for 28 GHz - Comparison between Analog Beamforming and
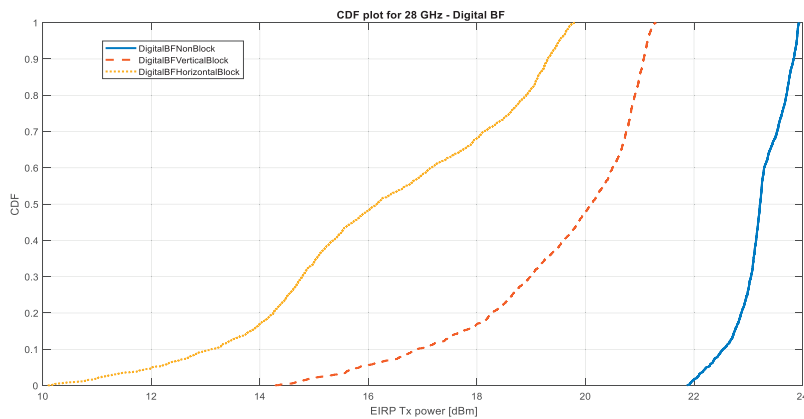Digital Beamforming

From Figure 9.30, we understood that the EIRP TX power is high for non-block case
compared to the block case in both digital and analog beamforming. In the analog
beamforming due to no antennas are placed at the bottom the EIRP TX power is low
compared to digital, this leads to very small coverage and possible call drop. In the
lower region, digital beamforming will have less chance of call drop with less EIRP TX
power that is digital beamforming with distributed antennas has better worst-case
performance compared to analog.

In summary: EIRP Tx power is calculated at (10% / 50%)

● Analog beamforming (non-blocking) – 16.8dBm / 22.8dBm (EIRP)
● Digital beamforming (non-blocking) – 22.5dBm / 23.2dBm (EIRP)
● Analog beamforming (Vertical blocking) – -4dBm / 15.35dBm (EIRP)
● Digital beamforming (Vertical blocking) – 16.91dBm / 20.11dBm (EIRP)
● Analog beamforming (Horizontal blocking) – 1.2dBm / 14.97dBm (EIRP)
● Digital beamforming (Horizontal blocking) – 13.01dBm / 16.14dBm (EIRP)

Therefore, it can be concluded that the maximum EIRP TX power is calculated as
27.76dBm for 28GHz from Chapter 8.

9.6.5 CDF plots for 39GHz – sub array based analog non-blocking and blocking case

Figure 9.31: CDF plot for 39 GHz - analog beamforming

From Figure 9.31, we understood that the EIRP TX power is high for non-block case compared to the block case. In the non-block case, all the 3 panel with 1X2 antenna elements are active and the EIRP TX power is 55% above the requirement level. By comparing the two block cases (vertical and horizontal) understood that almost 30% to 40% of the time analog beamforming in horizontal case is better than vertical case because no antenna panel is placed at the bottom of the mobile phone in vertical case whereas in horizontal only one antenna panel is blocked and will receive some signal power from the bottom. In this scenario it leads to less signal strength, small coverage, and possible call drops.

9.6.6 CDF plots for 39GHz – Distributed antenna element approach for digital
       beamforming - Non-Blocking and Blocking case
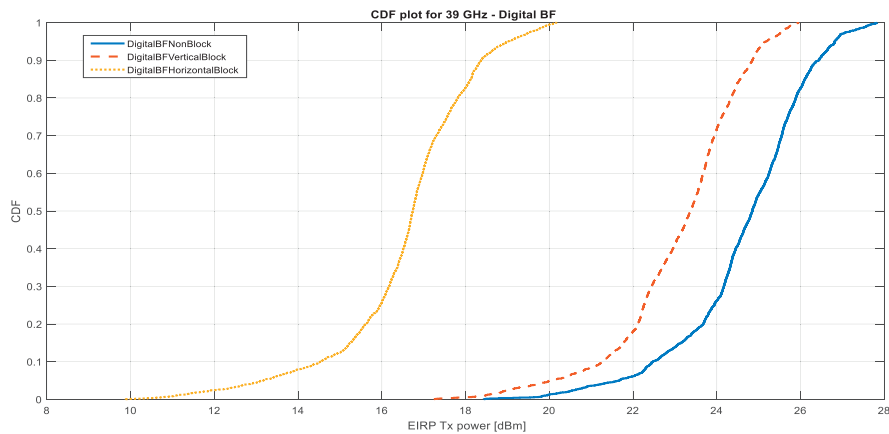
Figure 9.32: CDF plot for 39 GHz - digital beamforming

From Figure 9.32, we understood that the EIRP TX power is high for non-block case
compared to the block case. In the non-block case, all the 6 antenna elements were
active and distributed on the mobile phone unlike analog case. Whereas in blocking
cases, vertical holding is better than horizontal holding because in vertical case the
total number of block antenna is 1 and it is less compared to horizontal case with 4
blocked antenna elements. As seen from this mentioned figure, the EIRP TX power is
above 12dBm in 98% of cases in all situations.

9.6.7 CDF plots for 39GHz – Distributed antenna element approach for digital beamforming and sub array based analog beamforming- Non-Blocking case
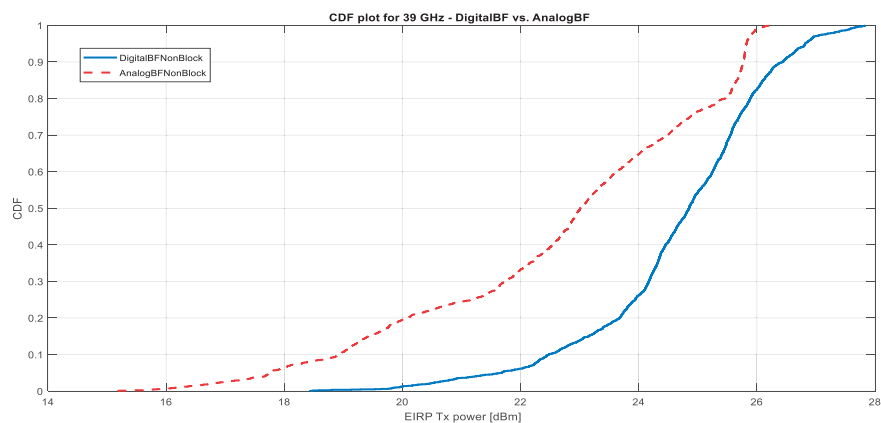
Figure 9.33: CDF plot for 39 GHz - Comparison between analog and digital BF (Non-Block)

As seen from the above plot in Figure 9.33, the digital non-blocking case outperformed the analog non-blocking case even though they have same antenna elements. Used 6 antennas with 3 panels in analog beamforming, the EIRP TX power is 35% less in most of the cases compared with 6 antenna elements in digital beamforming. For instance, if we use 7 antenna elements the digital beamforming TX power will be better in all the cases, but one need to think about the antenna/RF chip power consumption level, cost and size requirements.

In summary:

 EIRP TX power is calculated at (CDF 10% / CDF 50%)

● Analog beamforming (non-blocking) – 19dBm / 23.4dBm (EIRP)

● Digital beamforming (non-blocking) – 22.5dBm / 24.7dBm (EIRP)

9.6.8 CDF plots for 39GHz –Comparing all cases for distributed antenna element
approach for digital beamforming and sub array based analog beamforming
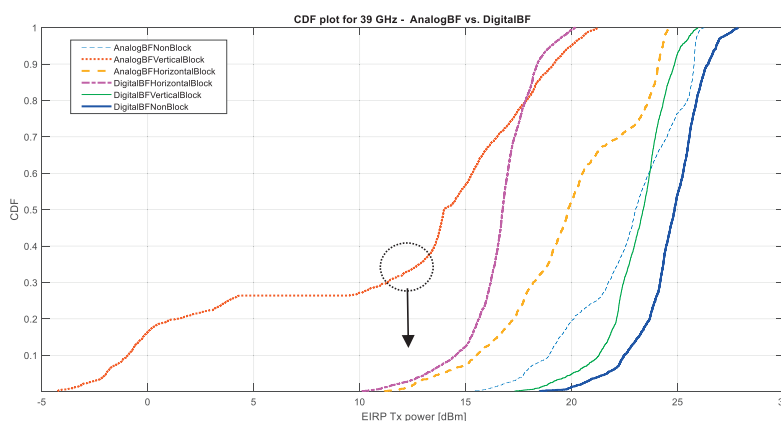
Figure 9.34: CDF plot for 39 GHz - Comparison between digital beamforming and
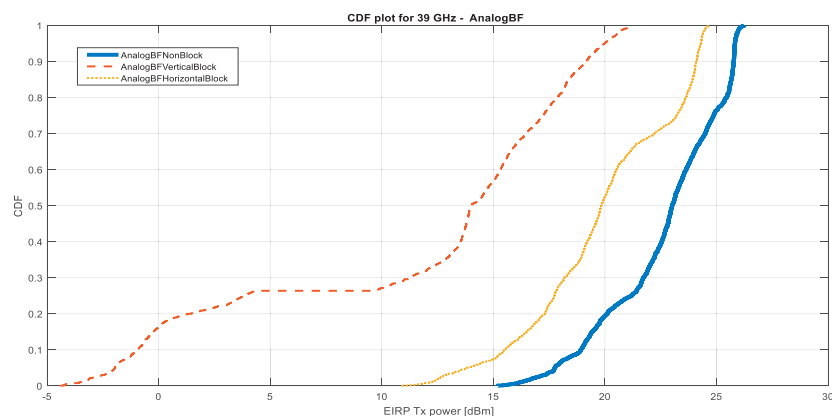analog beamforming

From Figure 9.34, we understood that the EIRP TX power is high for non-block case
compared to the block case in both digital and analog beamforming. In the analog
beamforming due to no antennas are placed at the bottom, the EIRP TX power is low
compared to digital, which leads to very small coverage and possibly a few call drops.
In the lower region, digital beamforming will have less chance of call drop with less
EIRP TX power, that is digital beamforming with distributed antennas has better
worst-case performance compared to analog.

In Summary: EIRP Tx power is calculated at (CDF 10% / CDF 50%)

- Analog beamforming (non-blocking) – 19dBm / 23.4dBm (EIRP)
- Digital beamforming (non-blocking) – 22.5dBm / 24.7dBm (EIRP)
- Analog beamforming (Vertical blocking) – -0.95dBm / 13.99dBm (EIRP)
- Digital beamforming (Vertical blocking) – 21.2dBm / 23.35dBm (EIRP)
- Analog beamforming (Horizontal blocking) – 15.5dBm / 19.83dBm (EIRP)
- Digital beamforming (Horizontal blocking) – 14.5dBm / 16.74dBm (EIRP)

Therefore, it can be concluded that the maximum EIRP TX power is calculated as
26.38dBm for 39GHz from Chapter 8.

Conclusion & Future work

By assessing the simulated results obtained from the antenna design, it can be observed that the patch antenna is resonating at 27.12 GHz and 39.06 GHz with bandwidths of 4.613 GHz and 8.873 GHz and gain values of 3.26 dBi and 1.88 dBi respectively. As a discussion for future work, a dual polarized patch antenna could be planned to design that corresponds to any orientation of polarization. Implementing this strategy may provide low cross-polarization levels with a wider impedance bandwidth.

One of the approaches to start implementing a dual polarized antenna would be adding notches/slots on the other edges of the patch, that help in increasing coupling. [17] (along with the current slot explained in Chapter 4). Attempts were made to design a dual polarized patch antenna which are interpreted below.
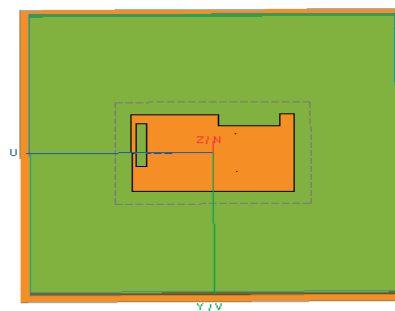

Figure 10.1: Patch antenna design trial with a notch added for dual polarization
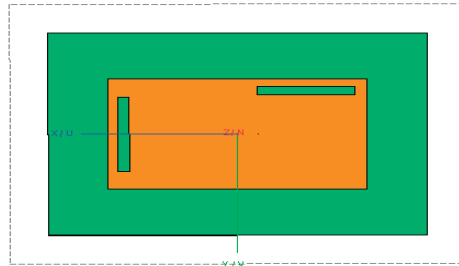
Figure 10.2: Patch antenna design trial with a rectangular slot added for dual polarization

In Figure 10.1 shown above, a notch is added and in Figure 10.2, a slot is added, both on the extreme top right edge of the patch antenna, or 90 degrees to the existing slot (on the left edge). The results obtained for the designs required a good impedance matching along with a wider reflection bandwidth at the desired resonant frequencies. Therefore, to obtain these parameters, betterment of the patch antenna design has to be made, maybe by altering the slot dimensions, increasing the feed port size [17] etc.

Advancing towards the simulated results in Figure 9.30 and Figure 9.34, it can be concluded that the distributed antenna element approach for digital beamforming could be a better choice for the existing sub array based analog beamforming radio architecture in the current mobile devices with respect to EIRP TX power and antenna placement flexibility. Having antennas placed in a distributed approach, the combining of antenna elements can be done from any direction (as discussed in Chapter 9) that provide a spherical and omnidirectional radiation with the help of beamforming, beam steering and beam tracking towards the whole sphere (ensuring to provide a good coverage), helps in incorporating fewer antennas in the mobile device, thus reducing the power consumption caused by each antenna and certainly the overall mmWave transceiver footprint.

With respect to the internal requirements set (mentioned in Chapter 8) and the simulated results obtained from Chapter 9, there is a need of at least 5 TX antennas placed in the mobile device in a distributed fashion for 28 GHz frequency, where the requirements of having an adequate omnidirectional coverage are very well fulfilled. With respect to the results seen for 39 GHz frequency, a minimum of 6 TX antennas are required, where about 96% of reasonable coverage is seen for a blocked-antenna scenario, which is yet better than the analog beamforming CDF distribution and fulfils the internal requirements.

Furthermore, as part of future work that can be planned for 39 GHz frequency, 7 or more TX antennas can be used to obtain an exceptional omnidirectional coverage, but as a trade-off point, adding more antennas assuredly increases the RF chip size, thereby requiring more power. In addition to this, re-designing of the proposed patch antenna can be envisioned (starting with Figures 10.1 and 10.2 shown), by investigating further on slots, and any required design calculations.

References

[1]   BeammWave AB, "Digital Beamforming Architectures The enabler of the Mass Market for 5G on mmWave Frequencies", September 2019. [Online]. Available: https://beammwave.com/download/73/?uid=86d13247 93

[2]   BeammWave AB, "Digital Beamforming for Mobile Devices The Power Efficient Architecture for 5G on mmWave Frequencies", September 2020. [Online]. Available: https://beammwave.com/download/69/?uid=30fff0131e

[3]   BeammWave AB, "Master Thesis Antenna design and link performance verification of Anntennas for mmWave handheld devices", September 2021. [Online]. Available: https://beammwave.com/career/

[4]   Yiming Huo, Xiaodai Dong, Wei Xu, "5G-and-Beyond-System-and-Hardware-Prototyping", 2018 IEEE 5G World Forum (5GWF), 2018, pp. 256-261, doi: 10.1109/5GWF.2018.8517059.

[5]   Yiming Huo, Xiaodai Dong, Wei Xu,"Design 5G Cellular User Equipment: From Theory to Practical Hardware"," in IEEE Access, vol. 5, pp. 13992-14010, 2017, doi: 10.1109/ACCESS.2017.2727550.

[6]   Lund University Online. (2020). ETEN10_1: Antenna Technology. [Online]. Available: https://canvas.education.lu.se/

[7]   Balanis, Constantine A. "Antenna Theory, Analysis and Design", 4th ed. Hoboken, NJ: John Wiley, 2016.

[8]   S. J. Orfanidis, "Electromagnetic Waves and Antennas", 2016 [Online]. Available: https://www.ece.rutgers.edu/~orfanidi/ewa/

[9]   *FEKO User's Manual,* Suite 7.0, EM Software & Systems-S.A. (Pty) Ltd, Stellenbosch 7600, South Africa, 2014.

[10]   "5G NR Frequency bands"**,** Wikipedia, Latest revision as of 05:47, 12 June 2022, https://en.wikipedia.org/wiki/5G_NR_frequency_bands

[11]   Surajo Muhammad, Abdulmalik S. Yaro, Isiyaku Ya'u, and A. S. Abubakar, "Design of single feed dual-band millimeter wave antenna for future 5g wireless applications", Science World Journal Vol 14(No 1) 2019, ISSN 1597-6343, Published by Faculty of Science, Kaduna State University

[12]   "Microstrip patch antenna parameters,FeedingTechniques,Shapes of the Patch", https://www.ijser.org/paper/Microstrip-Patch-Antenna-Parameters-Feeding-Techniques-and-Shape-of-the-Patch-A-Survey, in International Journal of Scientific & Engineering Research, Volume 6, Issue 4, April-2015,ISSN 2229-5518.

[13]   Bahare Mohamadzade, Raheel M Hashmi, Roy B V B Simorangkir, Reza Gharaei, Sabih Ur Rehman, Qammer H Abbasi, "Recent Advances in Fabrication Methods for Flexible Antennas in Wearable Devices: State of the Art", Sensors (Basel). 2019 May 19;19(10):2312. doi: 10.3390/s19102312. PMID: 31109158; PMCID: PMC6567739.

[14]   Link budget,"IWPC (Skyworks) 201906:5G Millimeter Wave Frequencies and Mobile Networks", pdf

[15]   Technical specification, "ETSI TS 138 101-2 V15.3.0 (2018-10), 5G; NR;User Equipment (UE) radio transmission and reception; Part 2: Range 2 Standalone(3GPP TS 38.101-2   version 15.3.0 Release 15)", pdf

[16]   "Spherical coordinate system", Wikipedia**,** Latest revision as of 01:17, 31 May 2022, https://en.wikipedia.org/wiki/Spherical_coordinate_system

[17]   Garg, Ramesh. "Microstrip Antenna Design Handbook". Boston, MA: Artech House, 2001.

Extended Material

_____

A.1 MatLab Code

A.1.1 SNR Detection

```
% First, estimate number of relevant paths

thr=0.05;  % threshold for inclusion of path. (linear in power)
for lm=1:length_timing_sync
path_power(:,lm)=sum(D(:,:,lm).^2,2);   %2 = 'c'
end
%  disp(size(path_power));
%  disp(size(ones(1,length_timing_sync)));
%  disp(max(path_power,[],2))
%  disp(path_power./max(path_power,[],2))
%  return
path_power=path_power./(max(path_power,[],2)*ones(1,length_timing_sync));
%,[],2) = 'c' when max
path_est=(path_power>thr);
for k=1:nT
for lm=1:length_timing_sync
D_path_est(k,:,lm)=D(k,:,lm)*(path_est(k,lm)==true);  % here is only estimated paths
non-zero
end
Dtot=D_path_est(:,:,1).^2;
for lm=2:length_timing_sync
Dtot=Dtot+(D(:,:,lm).^2);
end
```

```
[Dtotsort,Itot]=sort(Dtot,2,'descend');    %2 = 'c'
%'descend' means that we sort in descending order (we have the biggest
%first).
% ideal path estimator
%disp(Itot)
%disp(Dtotsort)
%return
%disp(phi_tt)
%disp(th_tt)

currently_used_antennas = zeros(nr_of_active_antennas, 2);

for indexactive = 1:nr_of_active_antennas
currently_used_antennas(indexactive,1) = Itot(index_use,indexactive);
%disp(Itot(index_use,indexactive));
end
%disp(currently_used_antennas);
for a_index=1:nr_of_active_antennas
 %this loop checks where each antenna taken from It ot (sorted by index
size)
 % is placed on the phone (atleast which side, not specific coords)
% we will use this information to know which antenna elements to highlight
in the 3d plot
if (currently_used_antennas(a_index,1) - Nf <= 0)
currently_used_antennas(a_index,2) = 1;        %second row will store nbr
1 => location = FRONT
elseif (currently_used_antennas(a_index,1) - Nf-Nb <= 0)
currently_used_antennas(a_index,2) = 2;        %second row will store nbr
2 => location = BACK
elseif (currently_used_antennas(a_index,1) - Nf-Nb-Nu <= 0)
currently_used_antennas(a_index,2) = 3;        %second row will store nbr
3 => location = TOP
elseif  (currently_used_antennas(a_index,1) - Nf-Nb-Nu-Nd <= 0)
currently_used_antennas(a_index,2) = 4;        %second row will store nbr
4 => location = BOT
elseif (currently_used_antennas(a_index,1) - Nf-Nb-Nu-Nd-Nr <= 0)
currently_used_antennas(a_index,2) = 5;        %second row will store nbr
5 => location = RIGHT
elseif (currently_used_antennas(a_index,1) - Nf-Nb-Nu-Nd-Nr-Nl <= 0)
currently_used_antennas(a_index,2) = 6;        %second row will store nbr
6 => location = LEFT
end
```

```
signal_decoder=0.001*ones(nT,nr_of_active_antennas);   % to not get -inf signals
strength if no correct path found
for k=1:nT
for lm=1:n_path
if (path_est(k,lm)==true)
signal_decoder(k,:)=max(0.001,signal_decoder(k,:)+signal_energy_captured(k,Itot(k
,[1:nr_of_active_antennas]),lm).*antenna_in_t(k,Itot(k,[1:nr_of_active_antennas]),l
m));
end
end
end
SNR_detector=sum(signal_decoder,2).^2.*10^(0.1*SNR);
% Signal to noise ratio in linear scale %2 = 'c'
```

A.1.2 Cutoff level measures

```
cut_off=110;
level= -50;
Mcutoff=A;
Mcutoff(:,3)=A(:,3).*(A(:,2)<cut_off)+level.*(A(:,2)>=cut_off);
A=Mcutoff;
save avalue A
```

A.1.3 CDF Plot

```
clear all;
close all;
load 'avalue.mat';
load 'SNR_temp.mat';
load 'SNR_temp_39ghz.mat';
% open the first Figure and plot on it
openfig('39GHz_digital_vertical_1.fig') ;
legend('off')
hold on
openfig('thirdfig_39ghz.fig');
legend('off')
hold on
A = 10*log10(SNR_detector);
B=sort(A);
Figure(10);
cdfplot(B);
xlabel(" EIRP Tx power [dBm]");
```

```
ylabel("CDF");
legend('DigitalBFnonblock','DigitalBFverticalblock','DigitalBFhorzblock');
title('CDF plot for 39 GHz -  DigitalBF ');
saveas(gcf,'39GHz_digital_Horiz_1.fig') ;
%saveas(gcf,'39GHz_analog_horizontal.fig') ;
close(gcf) ;
```

LUND
UNIVERSITY